GRHL2 enhances phosphorylated estrogen receptor DNA-binding and regulates ER-mediated transcriptional activation and repression

Running title: The role of GRHL2 in pS118-ER transcriptional activity

Rebecca M. Reese[a], Kyle T. Helzer[b], Kaelyn O. Allen[a], Christy Zheng[a], Natalia Solodin[a], Elaine T. Alarid[a]#

[a]McArdle Laboratory for Cancer Research, Department of Oncology and Carbone Comprehensive Cancer Center, University of Wisconsin – Madison, Madison WI

[b]Department of Human Oncology, University of Wisconsin – Madison, Madison WI

#Address correspondence to Elaine T. Alarid, alarid@oncology.wisc.edu

Data deposition: The data reported in this paper have been deposited in the Gene Expression Omnibus (GEO) database, www.ncbi.nlm.nih.gov/geo (accession number GSE202622).

Materials and Methods word count: 1996

Introduction, Results, Discussion word count: 3901

ABSTRACT

Phosphorylation of estrogen receptor α (ER) at serine 118 (pS118-ER) is induced by estrogen and is the most abundant post-translational mark associated with a transcriptionally active receptor. Cistromic analysis of pS118-ER from our group found enrichment of the GRHL2 motif near pS118-ER binding sites. In this report we use cistromic and transcriptomic analyses to interrogate the relationship between GRHL2 and pS118-ER. We found that GRHL2 is bound to chromatin at pS118-ER/GRHL2 co-occupancy sites prior to ligand treatment, and GRHL2 binding is required for maximal pS118-ER recruitment. pS118-ER/GRHL2 co-occupancy sites were enriched at active enhancers marked by H3K27ac and H3K4me1, along with FOXA1 and p300. Transcriptomic analysis yielded four subsets of ER/GRHL2 co-regulated genes revealing that GRHL2 can both enhance and antagonize E2-mediated ER transcriptional activity. Gene ontology analysis identified several coregulated genes involved in cell migration. Accordingly, knockdown of GRHL2 combined with estrogen treatment resulted in increased cell migration but no change in proliferation. These results support a model in which GRHL2 binds to select enhancers and facilitates pS118-ER recruitment to chromatin which then results in differential activation and repression of genes that control ER-positive breast cancer cell migration.

51 **INTRODUCTION**

52 Nuclear receptors are a class of transcription factors that modulate gene expression through
53 DNA interactions in response to stimuli such as steroid hormones. One such receptor is estrogen
54 receptor α (ER), which is expressed in over 70% of all breast cancers and is a major therapeutic target (1-
55 3). ER transcriptional activity is largely governed by the binding of its ligand, estrogen (E2), to the C-
56 terminus of the receptor (4, 5). Subsequently, the receptor binds to its consensus sequence, the
57 estrogen response element (ERE; 5′-GGTCAnnnTGACC-3′) (6, 7), and interacts with other coregulators
58 to modulate specific gene expression (8-10).

59 ER transcriptional activity can be altered by a variety of post-translational modifications (PTMs),
60 including phosphorylation of several residues (11). Of particular note is phosphorylation of the serine
61 118 residue (pS118-ER) in the N-terminus of the receptor which can be induced in both a ligand-
62 dependent and independent manner (12, 13). Clinically, pS118-ER is associated with low grade, well-
63 differentiated breast tumors (14, 15). Mutational analysis assessing the function of pS118 has found the
64 presence of pS118 is required for maximal E2-mediated ER transcriptional activity (16-18). Our group
65 recently completed a genome-wide analysis of pS118-ER DNA-binding sites and found pS118-ER
66 preferentially binds enhancers marked by H3K27ac in breast cancer cells (19). In addition, motif analysis
67 comparing sites bound by pS118-ER and ER without pS118 identified enrichment of the GRHL2 motif (5'-
68 AACCGGTT-3') (20-23) near pS118-ER binding sites (19). GRHL2 is a member of the Grainyhead-like
69 protein family (GRHL), a class of transcription factors which regulate epithelial differentiation (24-34).
70 GRHL2 has been implicated in a number of cancers, demonstrating both tumor suppressive and
71 oncogenic roles (35-54). The genomic analysis of pS118-ER DNA binding provided early evidence of
72 interplay between GRHL2 and ER in breast cancer cells.

73 There is increasing evidence that GRHL2 plays a role in facilitating ER transcriptional activity.
74 GRHL2 was identified as an ER interactor in rapid immunoprecipitation mass spectrometry of

75 endogenous protein (RIME) studies (55), and this interaction increases upon estrogen treatment (56).
76 Cistromic studies of ER and GRHL2 found that 29-35% of ER binding sites are co-occupied by a GRHL2
77 binding site (57, 58), indicating these two factors may function together to regulate gene transcription.
78 Studies suggest that GRHL2 acts through enhancer regions to facilitate the recruitment of MLL3, a lysine
79 methyltransferase responsible for depositing the enhancer marker H3K4me1 (58, 59). GRHL2 also co-
80 occupies chromatin with FOXA1, a pioneer factor associated with ER transcription, which promotes an
81 open chromatin structure and is found in regions marked by H3K4me1 (58, 60-63). GRHL2 chromatin-
82 binding can also be enhanced by E2 (19, 56) and E2-responsive GRHL2 binding sites are found more
83 frequently in enhancer regions identified by ER ChIA-Pet (56). Together with our work identifying the
84 enrichment of the GRHL2 motif near pS118-ER binding sites, this evidence supports a role for co-
85 regulation of gene expression by GRHL2 and ER at enhancer regions. We also found pS118-ER
86 preferentially binds near genes that are up-regulated by E2, suggesting GRHL2 may co-activate genes
87 with pS118-ER. However, GRHL2 can also suppress the production of enhancer RNAs (eRNA) at ER
88 enhancers for *GREB1*, *TFF1*, and *XBP1* (56), indicating that GRHL2 is also capable of repressing ER
89 transcriptional activity. The exact nature of the role of GRHL2 in modulating ER transcriptional activity,
90 more specifically pS118-ER transcriptional activity, and the biological processes co-regulated by both
91 factors are currently unclear.

92 In this report we examine the coordinate activities of GRHL2 and pS118-ER in the regulation of
93 gene expression in breast cancer cells using cistromic and transcriptomic approaches. Our data show
94 GRHL2 has a regulatory role in pS118-ER DNA binding at active enhancers, and GRHL2 can both activate
95 and repress pS118-ER target genes. We also found the combined activities of GRHL2 and pS118-ER
96 control the migratory behavior of breast cancer cells. These studies indicate a specific role for GRHL2 in
97 modulating pS118-ER transcriptional activity.

98 **MATERIALS AND METHODS**

99 **Cell culture**

100 MCF7, BT-474, SK-BR-3, MDA-MB-468, and MDA-MB-231 cells were maintained in 10% CO_2 at
101 37°C with high-glucose (4.5 g/L) Dulbecco's modified Eagles Medium (DMEM; Thermo Fisher,
102 #11965092) supplemented with 10% HyClone fetal bovine serum (FBS; Cytiva, #SH30910.03), 100 U/mL
103 penicillin 100 ug/mL streptomycin (1% Pen/Strep; Gibco, #15140-122), and 1 mM sodium pyruvate
104 (Gibco, #11360-070). T47D and ZR-75-1 cells were maintained in Roswell Park Memorial Institute 1640
105 (RPMI; Thermo Fisher, #11875-093) supplemented with 10% FBS and 1% Pen/Strep. BT-20 cells were
106 maintained in Minimum Essential Medium Alpha (MEMα; Thermo Fisher, #41061-029) supplemented
107 with 10% FBS and 1% Pen/Strep.

108 **Protein Preparation and Western Blot**

109 Protein samples were lysed in 1X Sample Buffer (62.5 mM Tris pH6.8, 2% SDS, 10% glycerol, 5%
110 β-mercaptoethanol) and subsequently boiled at 100°C for 10 minutes. Protein concentration for each
111 sample was quantified using the RC DC protein assay (Bio-Rad, #5000122) and 30-50 µg of protein were
112 run on a 10% SDS-PAGE gel. Proteins were transferred to a PVDF membrane (VWR, Cytiva, #10061-492),
113 blocked with 5% powdered milk in TBST (50 mM Tris-HCl pH7.4, 150 mM NaCl, 0.1% Tween-20), and
114 incubated overnight at 4°C in primary antibody. Primary antibodies used were ER (Santa Cruz
115 Biotechnology, #HC-20), pS118-ER (Abcam, #ab32396), GRHL1 (Santa Cruz Biotechnology, #sc-515541),
116 GRHL2 (Millipore Sigma, #HPA004820), GRHL3 (Santa Cruz Biotechnology, #sc-398838), β-actin
117 (Millipore Sigma, #A5441), and TBP (Thermo Fisher, #MA1-21516). Blots were incubated in secondary
118 antibody for one hour at room temperature (anti-rabbit; Amersham, #NA934) (anti-mouse; Amersham,
119 #NA931) and visualized with Clarity Western ECL Substrate (Bio-Rad, #1705061) on a ChemiDoc Imaging
120 System (Bio-Rad).

121 **Drug Treatments**

122 Prior to all drug treatments, cells were deprived of estrogens by culturing them in phenol-red
123 free DMEM or RPMI supplemented with 10% charcoal stripped FBS (ssDMEM/ssRPMI; Cytiva,
124 #SH30910.03, stripped in-house), 1% Pen/Strep, 2 mM L-glutamine (Thermo Fisher, #25030-081), and 1
125 mM sodium pyruvate (DMEM only) for three days. Cells were treated with vehicle (0.1% EtOH) or 10 nM
126 17β-estradiol (E2; Millipore Sigma #E2257). The duration of each treatment is noted for each
127 experiment.

128 **Knockdown of GRHL2 with siRNA**

129 For experiments involving GRHL2 knockdown, cells were reverse transfected with 25 nM of
130 either All Stars Negative control siRNA (siCtrl; QIAGEN, #1027280), siGRHL2 #1 (RNA-seq and qPCR
131 validation experiments) (Santa Cruz Biotechnology, #sc-77606), or siGRHL2 #2 (qPCR validation)
132 (Dharmacon, #L-014515-02-0050) using 2.5 ug/mL of Lipofectamine 2000 (Thermo Fisher Scientific,
133 #11668019) in Pen/Strep-free media.

134 **RNA Isolation and RT-qPCR**

135 RNA isolation was performed using the QIAGEN RNeasy Mini Kit (#74106) including treatment
136 with DNase (QIAGEN, #79254). Prior to qPCR, cDNA was generated using 1 µg of RNA and the iScript
137 cDNA Synthesis Kit (Bio-Rad, #1708891). qPCR was performed using iQ SYBR Green Supermix (Bio-Rad,
138 #1708884). Absolute quantification of RNA levels was performed by creating standard curves with
139 plasmids for *GRHL1* (Origene, #RC229312), *GRHL2* (Origene, #RG214498), and *GRHL3* (Origene,
140 #RC213012). The primers used were: *GRHL1*; Forward: 5'-ACAGCAAAAGAAACAGCATACCA-3' Reverse:
141 5'-TTGCCATGGGGAAGGACAAT-3'. *GRHL2*; Forward: 5'-GCCACCAAATCTCTCCGTCA-3' Reverse: 5'-
142 CCACCATCACCACACTCCTG-3'. *GRHL3*; Forward: 5'-TGCAAGCGAGGAATCTTAGTCA-3' Reverse: 5'-
143 CTCGAGAGGCCTTACAGCTC-3'. Relative RNA levels were calculated using the ΔΔCt method. The primers
144 used were: *LYPD3*; Forward: 5'-TCACCTTGACGGCAGCTAAT-3' Reverse: 5'- GAACCCTGGGCCTGTTACTC-3'.

145 *EFEMP1*: Forward: 5'-TTATCATGGCGGCTTCCGTT-3' Reverse 5'-TGGGCAAACACATCGGTTCT-3'.
146 *ARHGEF28*: Forward: 5'-TGGAAAACTGCTACAGGTCGT-3' Reverse 5'-ATGGCTTCTGATCAACGGCT-3'.
147 *SCUBE2*: Forward: 5'-TTCACCGCTCGGAAGAGGG-3' Reverse: 5'-TGGTTCTTGGCCAGCTCAAA-3'. *RPLP0*
148 (housekeeping gene): Forward: 5'-GACAATGGCAGCATCTACAAC-3' Reverse: 5'-
149 GCAGACAGACACTGGCAAC-3'.

150 **RNA-seq**

151 MCF7 cells and T47D cells were cultured in 10 cm plates in ssDMEM and ssRPMI, respectively,
152 for two days. On day three, cells were transfected as described above at a density of 200,000 cell/well in
153 12-well plates in Pen/Strep-free estrogen-deprived media. After 24 hours, media was changed to
154 estrogen-deprived media containing Pen/Strep and cells were treated with E2 or vehicle for 24 hours.
155 RNA was then isolated as described above. Samples for qPCR validation of RNA-seq were prepared using
156 the same process. Sequencing libraries were prepared using the Illumina TruSeq Stranded mRNA Library
157 Prep kit (Illumina, #20020595) and sequenced for 150bp paired-end reads on the NovaSeq6000 by the
158 Next Generation Sequencing department at the UW-Madison Biotechnology Center.

159 Quality control assessment of fastq files was performed using FASTQC (64). Adaptor trimming to
160 remove Illumina adaptors was performed using Cutadapt (65) through Trim Galore (66). Reads were
161 aligned to the hg38 genome with STAR (67). Aligned reads were assigned to genes using featureCounts
162 from the Subread package (68) and the hg38 NCBI RefSeq GTF (available at (69)) Differential gene
163 expression was performed using the DESeq2 package (70) with fold change shrinkage using ashr (71).
164 PCA plot was generated using DESeq2, heatmaps generated using pheatmap (72), and gene ontology
165 was performed using clusterProfiler (73).

166 **Migration Assays**

167 Migration assays were performed by seeding estrogen-deprived wild-type and CRISPR GRHL2
168 knockout cell pools obtained from Synthego (Menlo Park, CA) at a density of 700,000 cells/mL in Ibidi 4-

169 well dishes (Ibidi, #80406) simultaneously with vehicle or E2 treatment. 24 hours later, the 4 well insert
170 was removed to create a cell-free gap. The plates were imaged at 0 hours, 6 hours, and 24 hours, and
171 the gap was measured using the Wound Healing Size Tool plugin for imageJ (74).

172 **Cell Cycle Analysis**

173 Cells were deprived of estrogens for three days prior to adding treatments as described above
174 for 24h, 48h, and 72h. Cell pellets were fixed in 100% ethanol and then resuspended in a staining
175 solution consisting of 100 ug/mL RNase A (Invitrogen, #12091021) and 50 ug/mL propidium iodide
176 (Millipore Sigma, #P4170). The dye intensity of 10,000 events was captured on a Thermo Fisher Attune
177 NxT Flow Cytometer. Analysis was performed using the ModFit software.

178 **CUT&RUN**

179 MCF7 cells were cultured in 10cm plates in ssDMEM for one day. On day two, cells were
180 transfected as described above at a density of 350,000 cell/well in 6-well plates. After 24 hours, the
181 media was changed to the appropriate media containing Pen/Strep. The following day, cells were
182 removed from the plates using brief trypsinization and assessed for viability using trypan blue (Gibco,
183 #15250-061). $5x10^5$ viable cells were treated with vehicle or E2 for 30 min while rotating at 37°C.
184 Following treatment, samples were processed for CUT&RUN using the CUTANA ChIC/CUT&RUN Kit
185 (Epicypher, #14-1048; protocol from user manual version 2.0). Antibodies used were ER (Epicypher, #13-
186 2012), pS118-ER (Santa Cruz Biotechnology, #sc-12915), GRHL2 (Millipore Sigma, #HPA004820), and IgG
187 (Negative control; Epicypher, #13-0042).

188 DNA concentrations were measured using the Qubit dsDNA HS assay kit (Thermo Fisher,
189 #Q33231). Library prep was performed using the NEBNext Ultra II DNA Library Prep Kit for Illumina (NEB,
190 #E7103) and NEBNext Multiplex Oligos for Illumina (NEB, #E6440), with changes made to the protocol to
191 improve the capture of smaller TF fragments: the inactivation temperature after end-repair was
192 changed to 50°C for 1 hour, the bead size-selection ratio in the adaptor cleanup step was increased to

193 1.75x, and the bead size-selection ratio in the PCR cleanup step was increased to 1.2x (75, 76). Samples
194 were sequenced by paired-end 150bp sequencing on an Illumina NovaSeq 6000 by the Next Generation
195 Sequencing department at the UW-Madison Biotechnology Center.

196 Quality control assessment and adaptor trimming was performed as described in "RNA-seq".
197 Reads were aligned to the hg38 genome using Bowtie2 (77) using the --very-sensitive-local and --
198 dovetail flags. Aligned fragments were filtered for a maximum fragment length of 120bp using
199 alignmentSieve from Deeptools (78). Bam files from replicates were merged using Samtools merge.
200 Peaks were called with MACS2 (79) using IgG as a control and an FDR cutoff of 0.05. Peak overlaps were
201 performed with HOMER mergePeaks (80) with -d given. Heatmaps were plotted using Deeptools
202 computeMatrix and plotHeatmap.

203 **Generation of S118A ER mutation in MCF7 Cell Line**

204 Insertion of the S118A ER mutation in MCF7 cells was performed by following the Alt-R™
205 CRISPR-Cas9 System Protocol (IDT; Coralville, IA, USA) for use with the Neon™ Transfection System
206 (Thermo Fisher, #MPK5000) with alterations specific for MCF7 cells. MCF7 cells were brought up at a
207 low passage (p2) as recommended by the electroporation protocol. Cells were grown in DMEM
208 supplemented with 10% FBS and 1% Pen/Strep, split once, and then grown to confluency prior to cell
209 counting and electroporation. The crRNA:tracrRNA duplex was formed by resuspending the Alt-R™
210 CRISPR-Cas9 crRNA (5' – TGCAGGAAAGGCGACAGCTG – 3') and Alt-R™ CRISPR-Cas9 tracrRNA (IDT,
211 #1072532) in equimolar concentrations in nuclease-free IDTE buffer (10 mM Tris, 0.1 mM EDTA, pH 7.5;
212 IDT, #11-01-02-02) to a final duplex concentration of 44 µM. The mixture was brought to 95°C for 5 min
213 and allowed to cool to room temperature. To form the RNP complex, Alt-R™ S.p. Cas9 Nuclease 3NLS
214 (IDT, #1074181) was resuspended in Resuspension Buffer R (Thermo Fisher) to a final concentration of
215 36 µM. For each electroporation, equal volumes of the crRNA:tracrRNA duplex and RNP complex were
216 combined and incubated at room temp for 20 min. Prior to electroporation, MCF7 cells were collected,

217 washed with 1xPBS, counted, and resuspended in Resuspension Buffer R to a concentration of 5 x 10^6
218 cells/mL. 8 µL of the cell suspension was combined with the crRNA:tracrRNA:RNP complex, ssODN donor
219 (5 –CCCCCACTCAACAGCGTGTCTCCGAGCCCGCTGATGCTACTGCACCCGCCGCCGCAATTGGCGCCGTTCCTGC-
220 AGCCCCACGGCCAGCAGGTGCCCTACTACCTGGAGAACGAGCCCAGC – 3'), and Alt-R™ electroporation
221 enhancer (IDT, #1075915) for final concentrations of 1.8 µM crRNA:tracrRNA, 1.5 µM Cas9 RNP complex,
222 4 µM ssODN donor, and 1.8 µM electroporation enhancer. As a control, MCF7 cells with no
223 crRNA:tracrRNA were separately transfected keeping the same concentrations of the other components.
224 The final cell suspensions were electroporated using the Neon™ Transfection System with parameters
225 set for MCF7 cells (2 pulses, pulse voltage 1250v, pulse width 20ms). Cells were transferred to 12-well
226 plates with pre-warmed media without Pen/Strep and allowed to recover for 72 h.

227 **Screening of CRISPR-Cas9 clones**

228 After recovery, the cells were grown to confluency and cell populations were screened for
229 presence of the S118A mutation. DNA was isolated using the QIAGEN DNeasy Blood & Tissue Kit
230 (QIAGEN, #69504) and primers were generated to amplify around the region of interest (Forward: 5' –
231 GCCAACGCGCAGGTCTAC – 3'; Reverse: 5' – TCAAAGCGCCCCGTGTTTAT – 3'). Amplicons were subject to
232 digestion by SfoI (NEB, #R0606S) to test for the insertion of the S118A mutation. Populations positive for
233 SfoI digestion, indicating insertion of S118A mutation, underwent limiting dilution to identify single
234 colonies. Colonies were selected and expanded, followed by PCR screening and SfoI digestion as
235 described above. PCR amplicons from positive clones were additionally sequenced to confirm insertion
236 of the S118A mutation. Positive clones were further validated by induction of pS118-ER by E2 by
237 Western blot analysis, as described above.

238 **Chromatin Immunoprecipitation Sequencing (ChIP-seq)**

239 Cells were plated at a density of six million cells per 10cm plate with two plates per condition
240 and were deprived of estrogen for three days, followed by a 30-minute treatment with vehicle or E2.

241 Samples were prepared for ChIP as previously described (19) using a GRHL2 antibody (Millipore Sigma,
242 #HPA004820). DNA concentrations were measured using the Qubit dsDNA HS assay kit (Thermo Fisher,
243 #Q33231). Library prep was performed using the NEBNext Ultra II DNA Library Prep Kit for Illumina (NEB,
244 #E7103) and NEBNext Multiplex Oligos for Illumina (NEB, #E6440). Samples were sequenced by paired-
245 end 150bp sequencing on an Illumina NovaSeq 6000 by the Next Generation Sequencing department at
246 the UW-Madison Biotechnology Center.

247 Quality control assessment and adaptor trimming was performed as described in "RNA-seq".
248 Reads were aligned to the hg38 genome with Bowtie2 using --local and peaks were called with MACS2
249 using an FDR of 0.01. All peak file merging was performed using HOMER mergePeaks, -d given. For ChIP-
250 seq data from previous publications, data was downloaded using the SRA-Toolkit (81) from the following
251 accession numbers: pS118-ER/ER ChIP-seq (GSE117569) (19), GRHL2 ChIP-seq (GSE109820) (56), FOXA1
252 ChIP-seq (GSE59530) (82), p300 ChIP-seq (GSE60270) (83), H3K4me1/3 and H3K27ac ChIP-seq
253 (GSE57436) (84), and H3K27me3 ChIP-seq (GSE108787) (85). All data was trimmed and aligned using the
254 previously described methods with appropriate changes for single-end data. pS118-ER/ER and GRHL2
255 peaks were called using the narrowpeak setting in MACS2 with FDR cutoffs of 0.01 and 0.05,
256 respectively. Motif analysis was performed using annotatePeaks.pl and findMotifsGenome.pl from
257 HOMER.

258 **Statistical Methods**

259 The Wilcoxon rank sum test was used to analyze differences in RNA levels and percent gap
260 closure. A p-value less than 0.05 was considered significant.

261 **Data Availability**

262 The data reported in this paper have been deposited in the Gene Expression Omnibus (GEO)
263 database, www.ncbi.nlm.nih.gov/geo, under accession number GSE202622.

264 **RESULTS**

265 **GRHL2 expression is increased in ER-positive breast cancer compared to ER-negative**

266 The GRHL family is composed of three members, GRHL1, GRHL2, and GRHL3, all of which
267 regulate gene expression via the same DNA-binding motif (5'-AACCGGTT-3'). To characterize the GRHL
268 family in breast cancer, we first assessed the RNA expression of the GRHL family in normal breast tissue
269 and breast tumors using GEPIA2 (86). *GRHL2* expression was significantly increased in tumors than in
270 normal breast, whereas *GRHL1* and *GRHL3* showed no significant differences (Fig. 1A). These
271 observations were further supported by examination of TCGA datasets via cBioportal which showed that
272 *GRHL2* was amplified in 10.8% of breast cancers while *GRHL1* and *GRHL3* were amplified in less than 1%
273 of breast cancers (54, 87-90).

274 An important consideration in treating breast cancer is the ER status of the tumor. We assessed
275 protein and RNA expression of the GRHL family in four ER-positive breast cancer cell lines (MCF7, T47D,
276 ZR-75-1, BT-474), and four ER-negative cell lines (BT-20, SK-BR-3, MDA-MB-468, MDA-MB-231). Each of
277 the GRHL family members is expressed in all evaluated cell lines, with the exception of MDA-MB-231
278 which lacks GRHL2 expression (Fig. 1B,C). *GRHL2* mRNA expression was significantly higher in ER-positive
279 than ER-negative cell lines, whereas *GRHL1* and *GRHL3* expression did not differ significantly between
280 the two categories (Fig. 1B). These results were further corroborated by a representative immunoblot of
281 the GRHL family in breast cancer cell lines (Fig. 1C). A previous study in primary breast tumors also found
282 a significant correlation between GRHL2 and ER expression (40). Given the proclivity for GRHL2
283 expression in ER-positive breast cancer, we focused solely on GRHL2 for the remainder of our studies.

284 **pS118-ER/GRHL2 co-occupancy sites are found in enhancer regions**

285 In previous work from our group, we noted an enrichment of the GRHL2 motif near sites
286 occupied by ER phosphorylated at serine 118 (pS118-ER) (19). We asked whether there were differences
287 in the binding signals of pS118-ER/GRHL2 co-occupancy sites compared to those where each factor

288 occupies chromatin independently of the other. We took advantage of our own previously published
289 pS118-ER and ER ChIP-seq datasets (19) and a GRHL2 ChIP-seq performed in MCF7 cells treated with E2
290 for 30 and 45 minutes, respectively (56). The pS118-ER binding sites consist of a subset of sites within
291 the total ER binding sites. ER binding sites are defined as sites within the total ER binding set, excluding
292 those that are bound by pS118-ER. We identified 4,192 pS118-ER/GRHL2 co-occupancy sites and 4,028
293 ER/GRHL2 co-occupancy sites which comprise 28% and 12% of total pS118-ER and total ER binding sites,
294 respectively. Of the binding sites occupied independently by each factor, we identified 33,797 ER sites
295 (ER-only), 10,842 pS118-ER sites (pS118-ER-only), and 12,150 GRHL2 sites (GRHL2-only) (Fig. 2A). Of the
296 co-occupancy categories, GRHL2 binding was found prior to ligand treatment at 82.8% of the pS118-
297 ER/GRHL2 co-occupancy sites and 83.2% of the ER/GRHL2 co-occupancy sites, indicating GRHL2 can bind
298 the majority of these regions before E2-induced recruitment of ER (Fig. 2B). An example of a pS118-
299 ER/GRHL2 co-occupancy site is displayed in Fig. 2C. These results confirm GRHL2 is enriched at pS118-ER
300 binding sites relative to ER and indicate that GRHL2 and ER have both dependent and independent
301 functions.

302 To further probe the relationship of ER, pS118-ER, and GRHL2 occupancy sites, we examined the
303 signal intensity in the five binding categories. Binding signal of pS118-ER is substantially higher than ER
304 sites, emphasizing the importance of this PTM in ER DNA binding (Fig. 2D, column 1, orange vs blue
305 lines). However, the binding signal of pS118-ER and ER at regions co-occupied by GRHL2 did not appear
306 noticeably different from regions where GRHL2 binding is absent (Fig. 2D, columns 1 and 2, solid vs
307 dotted lines). Similarly, the presence of pS118-ER or ER does not substantially affect the binding signal of
308 GRHL2 (Fig. 2D, column 3, solid vs dotted lines). These data indicate ER/pS118-ER binding is not
309 preferentially stronger at GRHL2 binding sites and vice versa.

310 Previous studies showed GRHL2 can co-occupy chromatin with two factors that enhance ER
311 transcriptional activity: the pioneer factor FOXA1 (58, 63, 91) and p300, a histone acetyltransferase that

312 can deposit the enhancer histone mark H3K27ac (92, 93). We first asked whether the FOXA1 motif was
313 enriched at pS118-ER/GRHL2 co-occupancy sites. While the FOXA1 motif has comparable enrichment
314 across all categories with ER or pS118-ER binding, it is less prevalent at GRHL2-only binding sites (Fig.
315 3A), suggesting that FOXA1 could be preferentially recruited to sites occupied by both ER and GRHL2
316 over GRHL2 alone. Interestingly, the GRHL motif is the most prevalent motif at pS118-ER/GRHL2 and
317 ER/GRHL2 co-occupancy sites while the ERE is most prevalent at pS118-ER-only and ER-only sites (Fig.
318 3A). Next, we used previously published FOXA1 (82) and p300 (83) ChIP-seq studies performed in E2-
319 treated MCF7 cells (40 min and 1 hour treatments, respectively) to examine the presence of these two
320 factors at pS118-ER/GRHL2 co-occupancy sites (Fig. 3B). For both factors, the binding signal was
321 strongest at pS118-ER/GRHL2 co-occupancy sites followed by ER/GRHL2 co-occupancy sites and pS118-
322 ER-only sites (Fig. 3B). Analysis of the active enhancer marks H3K27ac and H3K4me1 ((84), 30 min
323 treatment), the promoter mark H3K4me3 ((84), 30 min treatment), and the repressive mark H3K27me3
324 ((85), 1 hour treatment) further revealed an enrichment of H3K27ac and H3K4me1 at pS118-ER/GRHL2
325 co-occupancy sites and ER/GRHL2 co-occupancy sites, relative to sites independently occupied by
326 pS118-ER, ER, or GRHL2 alone (Fig. 3B). The promotor mark H3K4me3 is enriched at GRHL2 only sites
327 relative to co-occupancy sites with pS118-ER and ER (Fig. 3B), which is consistent with the preferential
328 localization of GRHL2 only sites in promotor regions compared to any other binding category categories
329 (9.5% vs 2.5-5.5%) (Fig. 3B,C). The repressive H3K27me3 mark is weakest at pS118-ER/GRHL2 co-
330 occupancy sites followed by ER/GRHL2 co-occupancy sites (Fig. 3B). These data indicate pS118-
331 ER/GRHL2 co-occupancy sites are enriched at active enhancer regions.

332 **The loss of GRHL2 results in weaker pS118-ER DNA-binding**

333 Given the preference of pS118-ER/GRHL2 co-occupancy sites for enhancer regions compared to
334 either factor alone, we asked if GRHL2 is required for pS118-ER to bind to chromatin, and vice versa.
335 First, we assessed the requirement of GRHL2 for pS118-ER chromatin occupancy by performing

336 CUT&RUN for ER and pS118-ER in MCF7 cells depleted of GRHL2 using siRNA in the presence and
337 absence of E2 (Fig. 4A). There was no change in pS118-ER induction by E2 after depletion of GRHL2 (Fig.
338 4A). High-confidence pS118-ER binding sites were identified by removing peaks that were detected in
339 vehicle-treated cells and peaks that were not detected by the total ER antibody. In mock-transfected E2-
340 treated cells (siCtrl), we identified 7,269 total ER and 2,860 pS118-ER binding sites. After the depletion
341 of GRHL2, 4,171 ER sites were lost (57%) and 1,089 ER sites were gained. 3,098 ER sites were maintained
342 in both control and GRHL2-depleted conditions (Fig. 4B,C). Both total ER and pS118-ER binding signals
343 were substantially decreased in GRHL2-depleted cells, including instances when ER binding was
344 maintained in both control and GRHL2-depleted conditions (Fig. 4C). Phosphorylation of S118 could be
345 detected in control conditions at 1,178 (28.2%) of the ER binding sites that were lost and 2,026 (65.4%)
346 of ER binding sites that were maintained in both control and GRHL2-depleted conditions (Fig. 4B,C).
347 However, only 127 (11.7%) of new ER binding sites identified in GRHL2-depleted conditions were
348 phosphorylated at S118 (Fig. 4B,C). These data indicate GRHL2 is required for robust pS118-ER DNA
349 occupancy.

350 Conversely, to determine if the phosphorylation of S118 on ER is required for GRHL2 DNA-
351 binding, we performed ChIP-seq for GRHL2 in two independent MCF7 CRISPR knock-in cell lines in which
352 the serine at position 118 has been mutated to an alanine (S118A-ER), thereby preventing
353 phosphorylation at this site (Fig. 5A). In wild-type (WT) cells with intact pS118-ER, GRHL2 occupied
354 16,123 sites. In knock-in cell lines with S118A-ER, GRHL2 occupied 14,682 sites in one clone (S118A #1),
355 and 16,634 sites in the second clone (S118A #2). The majority of binding sites (13,066) were shared
356 among the three cell lines (Fig. 5B). Further, GRHL2 DNA-binding signal in the two S118A mutants was
357 comparable to the WT cells. Together, these data indicate that pS118-ER is not reciprocally required for
358 GRHL2 to bind DNA (Fig. 5C).

359 **GRHL2 and estrogen co-regulated genes are involved in cell migration**

360 After establishing that pS118-ER/GRHL2 co-occupancy sites bind preferentially in enhancer
361 regions and that GRHL2 is necessary for pS118-ER chromatin binding, we next investigated what genes
362 and biological processes these two factors co-regulate. To identify these genes, we performed RNA-seq
363 in triplicate in E2-treated MCF7 and T47D cells which had been depleted of GRHL2 using siRNA (Fig. 6A,
364 Supplemental Fig. 1A). E2 activation was confirmed by the induction of pS118-ER (12, 19) and
365 downregulation of total ER levels (94) (Fig. 6A, Supplemental Fig. 1A). As before, the loss of GRHL2 did
366 not affect E2-mediated pS118-ER induction (Fig. 6A, Supplemental Fig. 1A). Principle component analysis
367 (PCA) showed a large amount of variance between vehicle and E2 treatments in both cell lines, with a
368 larger variance observed in MCF7 cells (Fig. 6B, Supplemental Fig. 1B). There was a larger variance
369 between siCtrl and siGRHL2 in T47Ds than in MCF7s (Fig. 6B, Supplemental Fig. 1B). Differential
370 expression analysis was next performed using DESeq2 and the results were filtered for genes with an
371 adjusted p-value of less than 0.05 and a $\log_2$ fold change of greater than 1 or less than -1. Genes were
372 defined as primarily controlled by E2-activated ER (ER-only), primarily controlled by GRHL2 (GRHL2-
373 only), or co-regulated by both ER and GRHL2 (ER/GRHL2 co-regulated) (Fig. 6C, Supplemental Fig. 1C,
374 Supplemental Tables 1 and 2).

375 Examination of the ER/GRHL2 co-regulated genes revealed dual roles of GRHL2 in the regulation
376 of E2-mediated ER transcriptional activity. ER/GRHL2 co-regulated genes can be broken down into four
377 clusters (Fig. 6C,D, Supplemental Fig. 1C,D). When GRHL2 is lost, genes in clusters 1 and 4 show
378 increased downregulation and upregulation by estrogen, respectively. These data indicated that when
379 GRHL2 is present it opposes the regulatory action of ER on these genes. Genes in cluster 2 and 3 show
380 decreased downregulation and upregulation by ER when GRHL2 is lost. At these genes, when GRHL2 is
381 present it enhances ER transcriptional regulation. Using qRT-PCR and two independent siRNAs against
382 *GRHL2,* we validated these co-regulation patterns in a selection of genes: *LYPD3* (cluster 1), *EFEMP1*

383 (cluster 2), *ARHGEF28* (cluster 3), and *SCUBE2* (cluster 4) (Fig. 6E). Notably, *LYPD3* was previously
384 identified as a GRHL2 target gene in a tamoxifen resistant breast cancer cell line (63). These data
385 demonstrate that GRHL2 has pleiotropic effects on E2-induced pS118-ER transcriptional activity and can
386 work as either a transcriptional activator or repressor to influence the magnitude of estrogenic
387 responses in a gene-specific manner.

388 To determine which biological processes that ER/GRHL2 co-regulated genes may influence, we
389 performed gene ontology analysis using clusterProfiler. As expected, E2-only genes were primarily
390 associated with mitosis and cell cycle-related pathways (95) and GRHL2-only genes annotated to
391 epithelial terms such as "regulation of cell-cell adhesion" (24, 27, 31) and "wound healing" (96)
392 (Supplemental Table 3). Gene ontology analysis of ER/GRHL2 co-regulated genes found four of the top
393 ten most significant pathways in MCF7s were related to cell migration and motility (Fig. 7A,
394 Supplemental Table 3). To test the effect of E2-activate ER and GRHL2 on migration, we took advantage
395 of MCF7 cell pools which have undergone CRISPR-mediated depletion of GRHL2 (GRHL2-KO) (Fig. 7B-D).
396 Cells were treated with vehicle or E2 for 24 hours prior to the creation of a cell-free gap. GRHL2-KO cells
397 migrated across the cell-free gap more quickly than wild type (WT) cells over the course of 24 hours, and
398 migration was further enhanced by the addition of E2. We determined the increase in migration was not
399 a result of increased growth based on cell cycle analysis which indicated the loss of GRHL2 did not
400 impact E2-induced growth responses in this time frame (Fig. 7E). These data indicate a co-regulatory
401 role for GRHL2 and E2-induced pS118-ER in regulating cell migration. In addition, these data
402 demonstrate that GRHL2 is a critical blockade that inhibits the migratory properties of MCF7 cells in the
403 presence of activated ER.

404 **DISCUSSION**

405 Phosphorylation of S118 on the estrogen receptor is necessary for maximal ER-transcriptional
406 activity and chromatin-binding (12, 17, 19, 97). Our group identified a specific enrichment of the GRHL2

407 motif near pS118-ER occupancy sites suggesting an important role for GRHL2 in pS118-ER activity (19). In
408 this report we examined the co-dependency of GRHL2 and pS118-ER chromatin-occupancy and
409 transcriptional regulation of gene expression. We found that the loss of GRHL2 results in a global
410 decrease in pS118-ER chromatin-occupancy, demonstrating a critical role for GRHL2 in promoting
411 maximal pS118-ER recruitment to chromatin. GRHL2 can bind to chromatin prior to ligand treatment
412 and pS118-ER/GRHL2 co-occupancy sites tend to be localized to active enhancer regions marked by
413 H3K27ac and H3K4me1. Transcriptionally, GRHL2 can both enhance and antagonize E2-induced pS118-
414 ER transcriptional activity, indicating a role for GRHL2 in tuning pS118-ER-mediated gene expression.
415 These studies lead us to propose a model in which GRHL2 primes chromatin prior to ligand treatment to
416 facilitate the recruitment of pS118-ER and then further fine tunes E2-mediated pS118-ER transcriptional
417 activity through the recruitment or repression of additional coregulators (Fig. 8). The full range of
418 coregulators GRHL2 recruits or interacts with are still unknown and may vary based on the genetic
419 background of a given cell.

420 GRHL2 occupies sites destined to be co-bound by ER prior to E2-mediated ER activation, and
421 GRHL2 is necessary for robust pS118-ER DNA binding. In contrast, a S118A mutation in ER that prevents
422 phosphorylation failed to alter GRHL2 binding. These data suggest that GRHL2 primes enhancers for ER
423 binding events. Similar observations were made in studies of the highly conserved *Drosophila*
424 *melanogaster* homolog grainyhead (Grh) (98-101). These data have led to the hypothesis that the GRHL
425 family may function as pioneer factors, a specialized class of transcription factors that influence
426 transcriptional activity by promoting an open chromatin structure which promotes the recruitment of
427 other transcription factors (102, 103). Decreased Grh in the developing *D. melanogaster* and decreased
428 GRHL2 in epiblast-like cells resulted in a reduction of global chromatin accessibility (98, 99, 104). The
429 same was observed when all three mammalian GRHL family members were knocked down in MCF7 cells
430 (98). Another study using transgenic GFP reporters found Grh was bound to and promoted the

431 accessibility of various enhancer regions prior to their activation (98). Further, mutation of the Grh motif
432 at a selection of enhancers resulted in reduced chromatin accessibility (98). Interestingly, while the ERE
433 is typically the most highly enriched motif at pS118-ER occupancy sites (19), we instead discovered a
434 high prevalence of the GRHL motif at pS118-ER/GRHL2 co-occupancy sites. These data together suggest
435 that the presence of the GRHL motif may identify a select set of ER enhancers that require chromatin
436 opening in order for pS118-ER to bind DNA.

437 Previous studies have found GRHL2 can specifically associate with open and active enhancer
438 regions marked by H3K27ac and H3K4me1 (56, 104). In agreement, we observed an association of
439 GRHL2 binding sites with H3K27ac and H3K4me1 in breast cancer cells, particularly when it co-occupied
440 chromatin with ER or pS118-ER. A previous study examining co-occupancy sites of GRHL2 and androgen
441 receptor (AR), another nuclear receptor, also found an enrichment of H3K27ac at co-occupancy sites
442 compared to either factor alone (35). These data suggest that other transcription factors and
443 coregulators are needed in addition to GRHL2 to fully engage active enhancers. We also found the
444 strongest enrichment of FOXA1 binding signal at pS118-ER/GRHL2 co-occupancy sites. FOXA1 frequently
445 binds in active enhancer regions marked by H3K4me1 (62) and is known to facilitate ER recruitment to
446 chromatin (105). GRHL2 has been shown to work in concert with FOXA1 to recruit the histone
447 methyltransferase MLL3 which in turn deposits H3K4me1 (58). GRHL2 can also directly interact with
448 MLL3 via two amino acids in the GRHL2 transactivation domain, suggesting it may directly recruit MLL3
449 (106). However, regardless if MLL3 is present, GRHL2/FOXA1 co-occupancy sites also show stronger
450 enrichment of H3K4me1 than sites where either factor occupies chromatin individually (58). This
451 suggests that other coregulators may also contribute to H3K4me1 deposition at these sites. Overall, our
452 data provide additional evidence that the combination of GRHL2, FOXA1, and pS118-ER more faithfully
453 mark active enhancers than the individual factors.

454 Given the association of pS118-ER with upregulated genes (19) and the preference of GRHL2
455 and pS118-ER for active enhancers, we were surprised to find in our transcriptomic analysis that GRHL2
456 can both enhance and antagonize E2-mediated gene expression. This suggests that GRHL2 may interact
457 with other coregulators to modulate pS118-ER transcriptional function. As discussed above, these
458 factors likely include FOXA1 and MLL3, which are associated with marks of active enhancers. In this
459 report we found pS118-ER/GRHL2 co-occupancy sites display the strongest signal for the ER co-activator
460 p300 (93, 107), a histone acetyltransferase which can deposit the active enhancer mark H3K27ac (108).
461 Although p300 could be responsible for the presence of H3K27ac at pS118-ER/GRHL2 co-occupancy
462 sites, GRHL2 can inhibit p300 activity via an interaction of a 13 amino acid segment of the GRHL2 DNA
463 binding domain with the C-terminal end of p300 (92). Based on this finding, it is possible that GRHL2
464 could inhibit p300/ER transcriptional complexes leading to repression at select genes. Therefore, one
465 explanation of how GRHL2 can either activate or repress pS118-ER gene transcription is via GRHL2
466 activity on other transcription factors (FOXA1) or histone modifiers (MLL3, p300) that make up the
467 pS118-ER transcriptional complex.

468 In addition to exploring the interplay between GRHL2 and pS118-ER in chromatin binding, we
469 also wanted to understand what biological processes are co-regulated by GRHL2 and E2-activated
470 pS118-ER. As expected, genes associated with cell cycle and epithelial cell integrity aligned with ER-only
471 and GRHL-only gene sets respectively, consistent with their well-described roles (24, 27, 31, 95, 96).
472 Gene ontology analysis of ER/GRHL2 co-regulated genes, however, showed a large proportion of co-
473 regulated genes were involved in migration. We subsequently found that the loss of GRHL2 can increase
474 cell migration and this effect is further enhanced by the addition of E2. A previous study in ER-negative
475 cell lines also found GRHL2 influences migration in a tumor suppressive manner (40), but this study is
476 the first to show the co-regulatory role of GRHL2 and ER in this phenotype. In the hormone-dependent
477 ER-positive breast cancer model tested here, GRHL2 serves as an important blockade that inhibits cell

478 migration. An example of an ER/GRHL2 co-regulated gene that was annotated to cell migration in the
479 gene ontology analysis was *SASH1*, a tumor suppressor that inhibits invasion and migration (109, 110).
480 *SASH1* regulation is described by cluster 1, in which E2 downregulates *SASH1* and GRHL2 depletion
481 results in further downregulation of *SASH1* expression. Regulation of *SASH1* may be an example of an
482 instance where GRHL2 depletion results in an expression threshold being crossed and factors like SASH1
483 can no longer enact their tumor suppressive action, resulting in increased cell migration.

484 In summary, we have established a role for GRHL2 in facilitating the binding of pS118-ER to DNA
485 and have shown that sites co-occupied by GRHL2 and pS118-ER identify a set of enhancers marked by
486 H3K27ac and H3K4me1. We propose a model for the potential interactions among GRHL2, pS118-ER,
487 and other coregulators like p300 and FOXA1 to either complement or oppose pS118-ER transcriptional
488 activity. Finally, our data indicate that decreases in GRHL2 lead to increased cell migration that is further
489 enhanced by estrogen stimulation. These data identify dual activities of GRHL2 and its modulation of
490 activated ER and reveal a complexity to the interplay between GRHL2 and pS118-ER that impacts cancer
491 phenotypes, particularly migration.

492 **ACKNOWLEDGEMENTS**

493 We thank Kathryn Fox and the University of Wisconsin Carbone Comprehensive Cancer Center Flow
494 Cytometry Laboratory for their assistance with proliferation studies. We also thank Dr. David Lung for
495 his input into the manuscript. This work is supported by NIH grant R01 CA260140 to ETA.

496 **REFERENCES**

497 1. Green S, Walter P, Kumar V, Krust A, Bornert JM, Argos P, Chambon P. 1986. Human oestrogen
498 receptor cDNA: sequence, expression and homology to v-erb-A. Nature 320:134-9.
499 2. Sleightholm R, Neilsen BK, Elkhatib S, Flores L, Dukkipati S, Zhao R, Choudhury S, Gardner B,
500 Carmichael J, Smith L, Bennion N, Wahl A, Baine M. 2021. Percentage of Hormone Receptor
501 Positivity in Breast Cancer Provides Prognostic Value: A Single-Institute Study. J Clin Med Res
502 13:9-19.
503 3. Harvey JM, Clark GM, Osborne CK, Allred DC. 1999. Estrogen receptor status by
504 immunohistochemistry is superior to the ligand-binding assay for predicting response to
505 adjuvant endocrine therapy in breast cancer. J Clin Oncol 17:1474-81.

506 4. Tora L, White J, Brou C, Tasset D, Webster N, Scheer E, Chambon P. 1989. The human estrogen
507 receptor has two independent nonacidic transcriptional activation functions. Cell 59:477-87.
508 5. Webster NJ, Green S, Jin JR, Chambon P. 1988. The hormone-binding domains of the estrogen
509 and glucocorticoid receptors contain an inducible transcription activation function. Cell 54:199-
510 207.
511 6. Kumar V, Chambon P. 1988. The estrogen receptor binds tightly to its responsive element as a
512 ligand-induced homodimer. Cell 55:145-56.
513 7. Klein-Hitpass L, Ryffel GU, Heitlinger E, Cato AC. 1988. A 13 bp palindrome is a functional
514 estrogen responsive element and interacts specifically with estrogen receptor. Nucleic Acids Res
515 16:647-63.
516 8. Shiau AK, Barstad D, Loria PM, Cheng L, Kushner PJ, Agard DA, Greene GL. 1998. The structural
517 basis of estrogen receptor/coactivator recognition and the antagonism of this interaction by
518 tamoxifen. Cell 95:927-37.
519 9. Beato M, Sanchez-Pacheco A. 1996. Interaction of steroid hormone receptors with the
520 transcription initiation complex. Endocr Rev 17:587-609.
521 10. Heery DM, Kalkhoven E, Hoare S, Parker MG. 1997. A signature motif in transcriptional co-
522 activators mediates binding to nuclear receptors. Nature 387:733-6.
523 11. Le Romancer M, Poulard C, Cohen P, Sentis S, Renoir JM, Corbo L. 2011. Cracking the estrogen
524 receptor's posttranslational code in breast tumors. Endocr Rev 32:597-622.
525 12. Ali S, Metzger D, Bornert JM, Chambon P. 1993. Modulation of transcriptional activation by
526 ligand-dependent phosphorylation of the human oestrogen receptor A/B region. EMBO J
527 12:1153-60.
528 13. Bunone G, Briand PA, Miksicek RJ, Picard D. 1996. Activation of the unliganded estrogen
529 receptor by EGF involves the MAP kinase pathway and direct phosphorylation. EMBO J 15:2174-
530 83.
531 14. Sarwar N, Kim JS, Jiang J, Peston D, Sinnett HD, Madden P, Gee JM, Nicholson RI, Lykkesfeldt AE,
532 Shousha S, Coombes RC, Ali S. 2006. Phosphorylation of ERalpha at serine 118 in primary breast
533 cancer and in tamoxifen-resistant tumours is indicative of a complex role for ERalpha
534 phosphorylation in breast cancer progression. Endocr Relat Cancer 13:851-61.
535 15. Murphy L, Cherlet T, Adeyinka A, Niu Y, Snell L, Watson P. 2004. Phospho-serine-118 estrogen
536 receptor-alpha detection in human breast tumors in vivo. Clin Cancer Res 10:1354-9.
537 16. Cheng J, Zhang C, Shapiro DJ. 2007. A functional serine 118 phosphorylation site in estrogen
538 receptor-alpha is required for down-regulation of gene expression by 17beta-estradiol and 4-
539 hydroxytamoxifen. Endocrinology 148:4634-41.
540 17. Valley CC, Metivier R, Solodin NM, Fowler AM, Mashek MT, Hill L, Alarid ET. 2005. Differential
541 regulation of estrogen-inducible proteolysis and transcription by the estrogen receptor alpha N
542 terminus. Mol Cell Biol 25:5417-28.
543 18. Dutertre M, Smith CL. 2003. Ligand-independent interactions of p160/steroid receptor
544 coactivators and CREB-binding protein (CBP) with estrogen receptor-alpha: regulation by
545 phosphorylation sites in the A/B region depends on other receptor domains. Mol Endocrinol
546 17:1296-314.
547 19. Helzer KT, Szatkowski Ozers M, Meyer MB, Benkusky NA, Solodin N, Reese RM, Warren CL, Pike
548 JW, Alarid ET. 2019. The Phosphorylated Estrogen Receptor alpha (ER) Cistrome Identifies a
549 Subset of Active Enhancers Enriched for Direct ER-DNA Binding and the Transcription Factor
550 GRHL2. Mol Cell Biol 39.
551 20. Dynlacht BD, Attardi LD, Admon A, Freeman M, Tjian R. 1989. Functional analysis of NTF-1, a
552 developmentally regulated Drosophila transcription factor that binds neuronal cis elements.
553 Genes Dev 3:1677-88.

554 21. Wilanowski T, Tuckfield A, Cerruti L, O'Connell S, Saint R, Parekh V, Tao J, Cunningham JM, Jane
555 SM. 2002. A highly conserved novel family of mammalian developmental transcription factors
556 related to Drosophila grainyhead. Mech Dev 114:37-50.
557 22. Ming Q, Roske Y, Schuetz A, Walentin K, Ibraimi I, Schmidt-Ott KM, Heinemann U. 2018.
558 Structural basis of gene regulation by the Grainyhead/CP2 transcription factor family. Nucleic
559 Acids Res 46:2082-2095.
560 23. Ting SB, Caddy J, Hislop N, Wilanowski T, Auden A, Zhao LL, Ellis S, Kaur P, Uchida Y, Holleran
561 WM, Elias PM, Cunningham JM, Jane SM. 2005. A homolog of Drosophila grainy head is essential
562 for epidermal integrity in mice. Science 308:411-3.
563 24. Werth M, Walentin K, Aue A, Schonheit J, Wuebken A, Pode-Shakked N, Vilianovitch L, Erdmann
564 B, Dekel B, Bader M, Barasch J, Rosenbauer F, Luft FC, Schmidt-Ott KM. 2010. The transcription
565 factor grainyhead-like 2 regulates the molecular composition of the epithelial apical junctional
566 complex. Development 137:3835-45.
567 25. Ray HJ, Niswander LA. 2016. Grainyhead-like 2 downstream targets act to suppress epithelial-to-
568 mesenchymal transition during neural tube closure. Development 143:1192-204.
569 26. Rifat Y, Parekh V, Wilanowski T, Hislop NR, Auden A, Ting SB, Cunningham JM, Jane SM. 2010.
570 Regional neural tube closure defined by the Grainy head-like transcription factors. Dev Biol
571 345:237-45.
572 27. Pyrgaki C, Liu A, Niswander L. 2011. Grainyhead-like 2 regulates neural tube closure and
573 adhesion molecule expression during neural fold fusion. Dev Biol 353:38-49.
574 28. Walentin K, Hinze C, Werth M, Haase N, Varma S, Morell R, Aue A, Potschke E, Warburton D, Qiu
575 A, Barasch J, Purfurst B, Dieterich C, Popova E, Bader M, Dechend R, Staff AC, Yurtdas ZY, Kilic E,
576 Schmidt-Ott KM. 2015. A Grhl2-dependent gene network controls trophoblast branching
577 morphogenesis. Development 142:1125-36.
578 29. Narasimha M, Uv A, Krejci A, Brown NH, Bray SJ. 2008. Grainy head promotes expression of
579 septate junction proteins and influences epithelial morphogenesis. J Cell Sci 121:747-52.
580 30. Gao X, Bali AS, Randell SH, Hogan BL. 2015. GRHL2 coordinates regeneration of a polarized
581 mucociliary epithelium from basal stem cells. J Cell Biol 211:669-82.
582 31. Senga K, Mostov KE, Mitaka T, Miyajima A, Tanimizu N. 2012. Grainyhead-like 2 regulates
583 epithelial morphogenesis by establishing functional tight junctions through the organization of a
584 molecular network among claudin3, claudin4, and Rab25. Mol Biol Cell 23:2845-55.
585 32. Varma S, Mahavadi P, Sasikumar S, Cushing L, Hyland T, Rosser AE, Riccardi D, Lu J, Kalin TV,
586 Kalinichenko VV, Guenther A, Ramirez MI, Pardo A, Selman M, Warburton D. 2014. Grainyhead-
587 like 2 (GRHL2) distribution reveals novel pathophysiological differences between human
588 idiopathic pulmonary fibrosis and mouse models of pulmonary fibrosis. Am J Physiol Lung Cell
589 Mol Physiol 306:L405-19.
590 33. Adhikari N, Neupane S, Gwon GJ, Kim JY, An CH, Lee S, Sohn WJ, Lee Y, Kim JY. 2017. Grhl3
591 modulates epithelial structure formation of the circumvallate papilla during mouse
592 development. Histochem Cell Biol 147:5-16.
593 34. Mlacki M, Darido C, Jane SM, Wilanowski T. 2014. Loss of Grainy head-like 1 is associated with
594 disruption of the epidermal barrier and squamous cell carcinoma of the skin. PLoS One
595 9:e89247.
596 35. Paltoglou S, Das R, Townley SL, Hickey T, Tarulli G, Coutinho I, Fernandes RC, Hanson A, Denis I,
597 Carroll J, Dehm SM, Raj GV, Plymate S, Tilley WD, Selth LA. 2017. Novel androgen receptor co-
598 regulator GRHL2 exerts both oncogenic and anti-metastatic functions in prostate cancer. Cancer
599 Res doi:10.1158/0008-5472.CAN-16-1616.

600 36. Chung VY, Tan TZ, Tan M, Wong MK, Kuay KT, Yang Z, Ye J, Muller J, Koh CM, Guccione E, Thiery
601 JP, Huang RY. 2016. GRHL2-miR-200-ZEB1 maintains the epithelial status of ovarian cancer
602 through transcriptional regulation and histone modification. Sci Rep 6:19943.
603 37. Chen W, Yi JK, Shimane T, Mehrazarin S, Lin YL, Shin KH, Kim RH, Park NH, Kang MK. 2016.
604 Grainyhead-like 2 regulates epithelial plasticity and stemness in oral cancer cells. Carcinogenesis
605 37:500-10.
606 38. Pan X, Zhang R, Xie C, Gan M, Yao S, Yao Y, Jin J, Han T, Huang Y, Gong Y, Wang J, Yu B. 2017.
607 GRHL2 suppresses tumor metastasis via regulation of transcriptional activity of RhoG in non-
608 small cell lung cancer. Am J Transl Res 9:4217-4226.
609 39. Cieply B, Riley Pt, Pifer PM, Widmeyer J, Addison JB, Ivanov AV, Denvir J, Frisch SM. 2012.
610 Suppression of the epithelial-mesenchymal transition by Grainyhead-like-2. Cancer Res 72:2440-
611 53.
612 40. Werner S, Frey S, Riethdorf S, Schulze C, Alawi M, Kling L, Vafaizadeh V, Sauter G, Terracciano L,
613 Schumacher U, Pantel K, Assmann V. 2013. Dual roles of the transcription factor grainyhead-like
614 2 (GRHL2) in breast cancer. J Biol Chem 288:22993-3008.
615 41. Xiang J, Fu X, Ran W, Wang Z. 2017. Grhl2 reduces invasion and migration through inhibition of
616 TGFbeta-induced EMT in gastric cancer. Oncogenesis 6:e284.
617 42. Faddaoui A, Sheta R, Bachvarova M, Plante M, Gregoire J, Renaud MC, Sebastianelli A, Gobeil S,
618 Morin C, Ghani K, Bachvarov D. 2017. Suppression of the grainyhead transcription factor 2 gene
619 (GRHL2) inhibits the proliferation, migration, invasion and mediates cell cycle arrest of ovarian
620 cancer cells. Cell Cycle 16:693-706.
621 43. Yang X, Vasudevan P, Parekh V, Penev A, Cunningham JM. 2013. Bridging cancer biology with
622 the clinic: relative expression of a GRHL2-mediated gene-set pair predicts breast cancer
623 metastasis. PLoS One 8:e56195.
624 44. Nishino H, Takano S, Yoshitomi H, Suzuki K, Kagawa S, Shimazaki R, Shimizu H, Furukawa K,
625 Miyazaki M, Ohtsuka M. 2017. Grainyhead-like 2 (GRHL2) regulates epithelial plasticity in
626 pancreatic cancer progression. Cancer Med 6:2686-2696.
627 45. Kang X, Chen W, Kim RH, Kang MK, Park NH. 2009. Regulation of the hTERT promoter activity by
628 MSH2, the hnRNPs K and D, and GRHL2 in human oral squamous cell carcinoma cells. Oncogene
629 28:565-74.
630 46. Tanaka Y, Kanai F, Tada M, Tateishi R, Sanada M, Nannya Y, Ohta M, Asaoka Y, Seto M, Shiina S,
631 Yoshida H, Kawabe T, Yokosuka O, Ogawa S, Omata M. 2008. Gain of GRHL2 is associated with
632 early recurrence of hepatocellular carcinoma. J Hepatol 49:746-57.
633 47. Quan Y, Jin R, Huang A, Zhao H, Feng B, Zang L, Zheng M. 2014. Downregulation of GRHL2
634 inhibits the proliferation of colorectal cancer cells by targeting ZEB1. Cancer Biol Ther 15:878-87.
635 48. Quan Y, Xu M, Cui P, Ye M, Zhuang B, Min Z. 2015. [Expression and clinical significance of GRHL2
636 in colorectal cancer]. Zhonghua Zhong Liu Za Zhi 37:764-8.
637 49. Pawlak M, Kikulska A, Wrzesinski T, Rausch T, Kwias Z, Wilczynski B, Benes V, Wesoly J,
638 Wilanowski T. 2017. Potential Protective Role of Grainyhead-like Genes in the Development of
639 Clear Cell Renal Cell Carcinoma. Mol Carcinog doi:10.1002/mc.22682.
640 50. Butz H, Szabo PM, Nofech-Mozes R, Rotondo F, Kovacs K, Mirham L, Girgis H, Boles D, Patocs A,
641 Yousef GM. 2014. Integrative bioinformatics analysis reveals new prognostic biomarkers of clear
642 cell renal cell carcinoma. Clin Chem 60:1314-26.
643 51. Xiang J, Fu X, Ran W, Chen X, Hang Z, Mao H, Wang Z. 2013. Expression and role of grainyhead-
644 like 2 in gastric cancer. Med Oncol 30:714.
645 52. Torres-Reyes LA, Alvarado-Ruiz L, Pina-Sanchez P, Martinez-Silva MG, Ramos-Solano M, Olimon-
646 Andalon V, Ortiz-Lazareno PC, Hernandez-Flores G, Bravo-Cuellar A, Aguilar-Lemarroy A, Jave-

647 Suarez LF. 2014. Expression of transcription factor grainyhead-like 2 is diminished in cervical
648 cancer. Int J Clin Exp Pathol 7:7409-18.
649 53. Xiang X, Deng Z, Zhuang X, Ju S, Mu J, Jiang H, Zhang L, Yan J, Miller D, Zhang HG. 2013.
650 Correction: grhl2 determines the epithelial phenotype of breast cancers and promotes tumor
651 progression. PLoS One 8.
652 54. Reese RM, Harrison MM, Alarid ET. 2019. Grainyhead-like Protein 2: The Emerging Role in
653 Hormone-Dependent Cancers and Epigenetics. Endocrinology 160:1275-1288.
654 55. Mohammed H, D'Santos C, Serandour AA, Ali HR, Brown GD, Atkins A, Rueda OM, Holmes KA,
655 Theodorou V, Robinson JL, Zwart W, Saadi A, Ross-Innes CS, Chin SF, Menon S, Stingl J, Palmieri
656 C, Caldas C, Carroll JS. 2013. Endogenous purification reveals GREB1 as a key estrogen receptor
657 regulatory factor. Cell Rep 3:342-9.
658 56. Holding AN, Giorgi FM, Donnelly A, Cullen AE, Nagarajan S, Selth LA, Markowetz F. 2019.
659 VULCAN integrates ChIP-seq with patient-derived co-expression networks to identify GRHL2 as a
660 key co-regulator of ERa at enhancers in breast cancer. Genome Biol 20:91.
661 57. Chi D, Singhal H, Li L, Xiao T, Liu W, Pun M, Jeselsohn R, He H, Lim E, Vadhi R, Rao P, Long H,
662 Garber J, Brown M. 2019. Estrogen receptor signaling is reprogrammed during breast
663 tumorigenesis. Proc Natl Acad Sci U S A 116:11437-11443.
664 58. Jozwik KM, Chernukhin I, Serandour AA, Nagarajan S, Carroll JS. 2016. FOXA1 Directs H3K4
665 Monomethylation at Enhancers via Recruitment of the Methyltransferase MLL3. Cell Rep
666 17:2715-2723.
667 59. Heintzman ND, Stuart RK, Hon G, Fu Y, Ching CW, Hawkins RD, Barrera LO, Van Calcar S, Qu C,
668 Ching KA, Wang W, Weng Z, Green RD, Crawford GE, Ren B. 2007. Distinct and predictive
669 chromatin signatures of transcriptional promoters and enhancers in the human genome. Nat
670 Genet 39:311-8.
671 60. Cirillo LA, Lin FR, Cuesta I, Friedman D, Jarnik M, Zaret KS. 2002. Opening of compacted
672 chromatin by early developmental transcription factors HNF3 (FoxA) and GATA-4. Mol Cell
673 9:279-89.
674 61. Cirillo LA, McPherson CE, Bossard P, Stevens K, Cherian S, Shim EY, Clark KL, Burley SK, Zaret KS.
675 1998. Binding of the winged-helix transcription factor HNF3 to a linker histone site on the
676 nucleosome. EMBO J 17:244-54.
677 62. Lupien M, Eeckhoute J, Meyer CA, Wang Q, Zhang Y, Li W, Carroll JS, Liu XS, Brown M. 2008.
678 FoxA1 translates epigenetic signatures into enhancer-driven lineage-specific transcription. Cell
679 132:958-70.
680 63. Cocce KJ, Jasper JS, Desautels TK, Everett L, Wardell S, Westerling T, Baldi R, Wright TM, Tavares
681 K, Yllanes A, Bae Y, Blitzer JT, Logsdon C, Rakiec DP, Ruddy DA, Jiang T, Broadwater G, Hyslop T,
682 Hall A, Laine M, Phung L, Greene GL, Martin LA, Pancholi S, Dowsett M, Detre S, Marks JR,
683 Crawford GE, Brown M, Norris JD, Chang CY, McDonnell DP. 2019. The Lineage Determining
684 Factor GRHL2 Collaborates with FOXA1 to Establish a Targetable Pathway in Endocrine Therapy-
685 Resistant Breast Cancer. Cell Rep 29:889-903 e10.
686 64. FASTQC. https://www.bioinformatics.babraham.ac.uk/projects/fastqc/. Accessed May 7th,
687 2020.
688 65. Martin M. 2011. Cutadapt removes adapter sequences from high-throughput sequencing reads.
689 EMBnetjournal 17:10-12.
690 66. TrimGalore. https://github.com/FelixKrueger/TrimGalore. Accessed May 7th, 2020.
691 67. Dobin A, Davis CA, Schlesinger F, Drenkow J, Zaleski C, Jha S, Batut P, Chaisson M, Gingeras TR.
692 2013. STAR: ultrafast universal RNA-seq aligner. Bioinformatics 29:15-21.
693 68. Liao Y, Smyth GK, Shi W. 2014. featureCounts: an efficient general purpose program for
694 assigning sequence reads to genomic features. Bioinformatics 30:923-30.

695 69. NCBI. hg38 RefSeq GTF.
696 http://ftp.ensembl.org/pub/current_gtf/homo_sapiens/Homo_sapiens.GRCh38.104.gtf.gz.
697 Accessed November 10th, 2020.
698 70. Love MI, Huber W, Anders S. 2014. Moderated estimation of fold change and dispersion for
699 RNA-seq data with DESeq2. Genome Biol 15:550.
700 71. Stephens M. 2017. False discovery rates: a new deal. Biostatistics 18:275-294.
701 72. pheatmap. https://github.com/raivokolde/pheatmap. Accessed December 5th, 2020.
702 73. Wu T, Hu E, Xu S, Chen M, Guo P, Dai Z, Feng T, Zhou L, Tang W, Zhan L, Fu X, Liu S, Bo X, Yu G.
703 2021. clusterProfiler 4.0: A universal enrichment tool for interpreting omics data. Innovation (N
704 Y) 2:100141.
705 74. Suarez-Arnedo A, Torres Figueroa F, Clavijo C, Arbelaez P, Cruz JC, Munoz-Camargo C. 2020. An
706 image J plugin for the high throughput image analysis of in vitro scratch wound healing assays.
707 PLoS One 15:e0232565.
708 75. Liu N, Hargreaves VV, Zhu Q, Kurland JV, Hong J, Kim W, Sher F, Macias-Trevino C, Rogers JM,
709 Kurita R, Nakamura Y, Yuan GC, Bauer DE, Xu J, Bulyk ML, Orkin SH. 2018. Direct Promoter
710 Repression by BCL11A Controls the Fetal to Adult Hemoglobin Switch. Cell 173:430-442 e17.
711 76. Zhu Q, Liu N, Orkin SH, Yuan GC. 2019. CUT&RUNTools: a flexible pipeline for CUT&RUN
712 processing and footprint analysis. Genome Biol 20:192.
713 77. Langmead B, Salzberg SL. 2012. Fast gapped-read alignment with Bowtie 2. Nat Methods 9:357-
714 9.
715 78. Ramirez F, Ryan DP, Gruning B, Bhardwaj V, Kilpert F, Richter AS, Heyne S, Dundar F, Manke T.
716 2016. deepTools2: a next generation web server for deep-sequencing data analysis. Nucleic
717 Acids Res 44:W160-5.
718 79. Zhang Y, Liu T, Meyer CA, Eeckhoute J, Johnson DS, Bernstein BE, Nusbaum C, Myers RM, Brown
719 M, Li W, Liu XS. 2008. Model-based analysis of ChIP-Seq (MACS). Genome Biol 9:R137.
720 80. Heinz S, Benner C, Spann N, Bertolino E, Lin YC, Laslo P, Cheng JX, Murre C, Singh H, Glass CK.
721 2010. Simple combinations of lineage-determining transcription factors prime cis-regulatory
722 elements required for macrophage and B cell identities. Mol Cell 38:576-89.
723 81. SRA-Toolkit. https://trace.ncbi.nlm.nih.gov/Traces/sra/sra.cgi?view=software. Accessed April
724 21st, 2020.
725 82. Franco HL, Nagari A, Kraus WL. 2015. TNFalpha signaling exposes latent estrogen receptor
726 binding sites to alter the breast cancer cell transcriptome. Mol Cell 58:21-34.
727 83. Liu Z, Merkurjev D, Yang F, Li W, Oh S, Friedman MJ, Song X, Zhang F, Ma Q, Ohgi KA, Krones A,
728 Rosenfeld MG. 2014. Enhancer activation requires trans-recruitment of a mega transcription
729 factor complex. Cell 159:358-73.
730 84. Brunelle M, Nordell Markovits A, Rodrigue S, Lupien M, Jacques PE, Gevry N. 2015. The histone
731 variant H2A.Z is an important regulator of enhancer activity. Nucleic Acids Res 43:9742-56.
732 85. Zhou Y, Gerrard DL, Wang J, Li T, Yang Y, Fritz AJ, Rajendran M, Fu X, Stein G, Schiff R, Lin S,
733 Frietze S, Jin VX. 2019. Temporal dynamic reorganization of 3D chromatin architecture in
734 hormone-induced breast cancer and endocrine resistance. Nat Commun 10:1522.
735 86. Tang Z, Li C, Kang B, Gao G, Li C, Zhang Z. 2017. GEPIA: a web server for cancer and normal gene
736 expression profiling and interactive analyses. Nucleic Acids Res 45:W98-W102.
737 87. Kotarba G, Taracha-Wisniewska A, Wilanowski T. 2020. Grainyhead-like transcription factors in
738 cancer - Focus on recent developments. Exp Biol Med (Maywood) 245:402-410.
739 88. Hoadley KA, Yau C, Hinoue T, Wolf DM, Lazar AJ, Drill E, Shen R, Taylor AM, Cherniack AD,
740 Thorsson V, Akbani R, Bowlby R, Wong CK, Wiznerowicz M, Sanchez-Vega F, Robertson AG,
741 Schneider BG, Lawrence MS, Noushmehr H, Malta TM, Cancer Genome Atlas N, Stuart JM, Benz

742 CC, Laird PW. 2018. Cell-of-Origin Patterns Dominate the Molecular Classification of 10,000
743 Tumors from 33 Types of Cancer. Cell 173:291-304 e6.
744 89. Cerami E, Gao J, Dogrusoz U, Gross BE, Sumer SO, Aksoy BA, Jacobsen A, Byrne CJ, Heuer ML,
745 Larsson E, Antipin Y, Reva B, Goldberg AP, Sander C, Schultz N. 2012. The cBio cancer genomics
746 portal: an open platform for exploring multidimensional cancer genomics data. Cancer Discov
747 2:401-4.
748 90. Gao J, Aksoy BA, Dogrusoz U, Dresdner G, Gross B, Sumer SO, Sun Y, Jacobsen A, Sinha R,
749 Larsson E, Cerami E, Sander C, Schultz N. 2013. Integrative analysis of complex cancer genomics
750 and clinical profiles using the cBioPortal. Sci Signal 6:pl1.
751 91. Hurtado A, Holmes KA, Ross-Innes CS, Schmidt D, Carroll JS. 2011. FOXA1 is a key determinant of
752 estrogen receptor function and endocrine response. Nat Genet 43:27-33.
753 92. Pifer PM, Farris JC, Thomas AL, Stoilov P, Denvir J, Smith DM, Frisch SM. 2016. Grainyhead-like 2
754 inhibits the coactivator p300, suppressing tubulogenesis and the epithelial-mesenchymal
755 transition. Mol Biol Cell 27:2479-92.
756 93. Hanstein B, Eckner R, DiRenzo J, Halachmi S, Liu H, Searcy B, Kurokawa R, Brown M. 1996. p300
757 is a component of an estrogen receptor coactivator complex. Proc Natl Acad Sci U S A 93:11540-
758 5.
759 94. Alarid ET, Bakopoulos N, Solodin N. 1999. Proteasome-mediated proteolysis of estrogen
760 receptor: a novel component in autologous down-regulation. Mol Endocrinol 13:1522-34.
761 95. Prall OW, Rogan EM, Sutherland RL. 1998. Estrogen regulation of cell cycle progression in breast
762 cancer cells. J Steroid Biochem Mol Biol 65:169-74.
763 96. Boglev Y, Wilanowski T, Caddy J, Parekh V, Auden A, Darido C, Hislop NR, Cangkrama M, Ting SB,
764 Jane SM. 2011. The unique and cooperative roles of the Grainy head-like transcription factors in
765 epidermal development reflect unexpected target gene specificity. Dev Biol 349:512-22.
766 97. Kato S, Endoh H, Masuhiro Y, Kitamoto T, Uchiyama S, Sasaki H, Masushige S, Gotoh Y, Nishida E,
767 Kawashima H, Metzger D, Chambon P. 1995. Activation of the estrogen receptor through
768 phosphorylation by mitogen-activated protein kinase. Science 270:1491-4.
769 98. Jacobs J, Atkins M, Davie K, Imrichova H, Romanelli L, Christiaens V, Hulselmans G, Potier D,
770 Wouters J, Taskiran, II, Paciello G, Gonzalez-Blas CB, Koldere D, Aibar S, Halder G, Aerts S. 2018.
771 The transcription factor Grainy head primes epithelial enhancers for spatiotemporal activation
772 by displacing nucleosomes. Nat Genet 50:1011-1020.
773 99. Nevil M, Bondra ER, Schulz KN, Kaplan T, Harrison MM. 2017. Stable Binding of the Conserved
774 Transcription Factor Grainy Head to its Target Genes Throughout Drosophila melanogaster
775 Development. Genetics 205:605-620.
776 100. Nevil M, Gibson TJ, Bartolutti C, Iyengar A, Harrison MM. 2020. Establishment of chromatin
777 accessibility by the conserved transcription factor Grainy head is developmentally regulated.
778 Development 147.
779 101. Potier D, Davie K, Hulselmans G, Naval Sanchez M, Haagen L, Huynh-Thu VA, Koldere D, Celik A,
780 Geurts P, Christiaens V, Aerts S. 2014. Mapping gene regulatory networks in Drosophila eye
781 development by large-scale transcriptome perturbations and motif inference. Cell Rep 9:2290-
782 303.
783 102. Magnani L, Eeckhoute J, Lupien M. 2011. Pioneer factors: directing transcriptional regulators
784 within the chromatin environment. Trends Genet 27:465-74.
785 103. Zaret KS, Carroll JS. 2011. Pioneer transcription factors: establishing competence for gene
786 expression. Genes Dev 25:2227-41.
787 104. Chen AF, Liu AJ, Krishnakumar R, Freimer JW, DeVeale B, Blelloch R. 2018. GRHL2-Dependent
788 Enhancer Switching Maintains a Pluripotent Stem Cell Transcriptional Subnetwork after Exit
789 from Naive Pluripotency. Cell Stem Cell doi:10.1016/j.stem.2018.06.005.

790 105. Carroll JS, Liu XS, Brodsky AS, Li W, Meyer CA, Szary AJ, Eeckhoute J, Shao W, Hestermann EV,
791 Geistlinger TR, Fox EA, Silver PA, Brown M. 2005. Chromosome-wide mapping of estrogen
792 receptor binding reveals long-range regulation requiring the forkhead protein FoxA1. Cell
793 122:33-43.
794 106. MacFawn I, Wilson H, Selth LA, Leighton I, Serebriiskii I, Bleackley RC, Elzamzamy O, Farris J, Pifer
795 PM, Richer J, Frisch SM. 2019. Grainyhead-like-2 confers NK-sensitivity through interactions with
796 epigenetic modifiers. Mol Immunol 105:137-149.
797 107. Kraus WL, Kadonaga JT. 1998. p300 and estrogen receptor cooperatively activate transcription
798 via differential enhancement of initiation and reinitiation. Genes Dev 12:331-42.
799 108. Martire S, Nguyen J, Sundaresan A, Banaszynski LA. 2020. Differential contribution of p300 and
800 CBP to regulatory element acetylation in mESCs. BMC Mol Cell Biol 21:55.
801 109. Martini M, Gnann A, Scheikl D, Holzmann B, Janssen KP. 2011. The candidate tumor suppressor
802 SASH1 interacts with the actin cytoskeleton and stimulates cell-matrix adhesion. Int J Biochem
803 Cell Biol 43:1630-40.
804 110. Jiang K, Liu P, Xu H, Liang D, Fang K, Du S, Cheng W, Ye L, Liu T, Zhang X, Gong P, Shao S, Wang Y,
805 Meng S. 2020. SASH1 suppresses triple-negative breast cancer cell invasion through YAP-
806 ARHGAP42-actin axis. Oncogene 39:5015-5030.

807

808 **FIGURE LEGENDS**

809 **Figure 1: GRHL2 expression is higher in ER-positive vs ER-negative breast cancer.** A) mRNA expression
810 of the *GRHL* family in normal and tumor breast tissue obtained from GEPIA2. A * indicates a p-value <
811 0.05. B) Absolute quantification of *GRHL* mRNA and in a panel of ER-positive and ER-negative breast
812 cancer cell lines. Error bars represent mean ± standard error. C) Representative Western blot of GRHL
813 protein levels in the same cell panel. β-actin is used as a loading control.

814 **Figure 2: Identification of pS118-ER/GRHL2 co-occupancy sites.** A) Venn diagram showing the overlap
815 of MCF7 E2-treated total ER, pS118-ER, and GRHL2 ChIP-seq datasets. pS118-ER binding sites are a
816 subset of total ER bindings sites. ER sites are defined as those that do not overlap with the pS118-ER
817 dataset. Five binding categories were established: pS118-ER/GRHL2 co-occupancy (4,192 sites),
818 ER/GRHL2 co-occupancy (4,028 sites), pS118-ER-only (10,842 sites), ER-only (33,797 sites), and GRHL2-
819 only (12,150 sites). B) Venn diagrams showing the overlap of pS118-ER/GRHL2 co-occupancy sites and
820 ER/GRHL2 co-occupancy sites with GRHL2 peaks detected in vehicle conditions. C) Representative
821 genome browser track of a pS118-ER/GRHL2 co-occupancy site. D) Heatmaps showing binding signal of

822 ER, pS118-ER, and GRHL2 at each of the five binding categories. Data were obtained from previously
823 published ChIP-seq datasets (56).

824 **Figure 3: pS118-ER/GRHL2 co-occupancy sites are located at enhancers.** A) Motif analysis of the GRHL,
825 ERE, and FOXA1 motifs at co-occupancy sites. The first column shows enrichment of the indicated motif
826 (ERE in blue, GRHL in green, FOXA1 in purple) relative to the peak center. The second column shows the
827 percent of sites with each of the motifs. C) Heatmaps showing binding signal of FOXA1 and p300 and
828 metaplots showing the signal of the histone modifications H3K4me1, H3K4me3, H3K27ac, and
829 H3K27me3 at each of the previously established binding categories. Data were obtained from previously
830 published ChIP-seq datasets (82-85). C) Genome location annotation of the five binding categories. Sites
831 were annotated to introns, intergenic regions, promoters, exons, or other. Promoters were defined as -
832 1kb to +100bp from the transcription start site.

833 **Figure 4: The loss of GRHL2 causes a reduction in ER and pS118-ER chromatin binding.** A)
834 Representative western blot of MCF7 samples used in CUT&RUN experiments. Cells were transfected
835 with siCtrl or siGRHL2 and treated for 30 minutes with vehicle or 10 nM E2. β-actin is used as a loading
836 control. B) Venn diagram and upset plot indicating the overlap of ER and pS118-ER CUT&RUN peaks in
837 E2-treated, siCtrl- or siGRHL2-transfected cells. C) Heatmaps showing CUT&RUN signal for ER, pS118-ER,
838 and GRHL2 at lost ER sites (purple), maintained ER siCtrl/siGRHL2 sites (purple and green dashed), and
839 gained ER sites (green). The percent of ER sites detected by the pS118-ER antibody are indicated in
840 region labels.

841 **Figure 5: Loss of pS118-ER does not affect GRHL2 chromatin binding.** A) Representative western blot of
842 WT and S118A mutant MCF7 cells used for ChIP-seq. Cells were treated for 30min with vehicle or 10 nM
843 E2. TBP is used as a loading control. B) Venn diagrams showing the overlap of E2 GRHL2 binding sites

844 between WT cells and two S118A mutant clones. C) Heatmaps showing GRHL2 binding signal at
845 collective GRHL2 binding sites across all three cell lines.

846 **Figure 6: GRHL2 can enhance and antagonize E2-mediated ER transcriptional activity.** A)
847 Representative Western blot of MCF7 samples used in RNA-seq. Cells were transfected with siCtrl or
848 siGRHL2 and treated for 24 hours with vehicle or 10 nM E2. β-actin is used as a loading control. B) PCA
849 plot of MCF7 RNA-seq data displaying differences between siCtrl (purple), siGRHL2 (green), vehicle
850 treatment (circles), and E2 treatment (triangles). C) Heatmap showing the expression of ER/GRHL2 co-
851 regulated genes, ER-only regulated genes, and GRHL2-only regulated genes. D) Gene expression profiles
852 of ER/GRHL2 co-regulated gene clusters. Error bars represent mean ± standard error. E) qPCR validation
853 of selected genes from each of the ER/GRHL2 co-regulated gene clusters using two different siRNAs
854 against *GRHL2*. All values are relative to siCtrl Veh. Error bars represent mean ± standard error.

855 **Figure 7: GRHL2 and E2 co-regulate migration.** A) Gene ontology analysis for biological processes
856 performed with clusterProfiler on ER/GRHL2 co-regulated genes. Terms related to cell migration,
857 motility, and locomotion are highlighted in red. The size of the dots represents the number of genes
858 annotated to a given term, and color represents the adjusted p-value with red being the most
859 significant. B) Brightfield images of WT and GRHL2-KO cell migration across a cell-free gap over the
860 course of 24 hours. C) Representative Western blot showing the loss of GRHL2 in pooled CRISPR GRHL2-
861 KO cells. D) Quantification of the percent gap closure over 6 hours and 24 hours. Error bars represent
862 mean ± standard error and * indicates a p-value < 0.05. E) Flow cytometry analysis showing the percent
863 of cells in each of the cell cycle stages (S, G2, G1). WT and GRHL2-KO cells were treated with vehicle or
864 10 nM E2 over 24h, 48h, and 72h. Error bars represent mean ± standard error.

865 **Figure 8: Model of GRHL2 function in facilitating pS118-ER binding and transcriptional activity.** GRHL2
866 binds to the GRHL motif in enhancers prior to ligand treatment. Upon exposure to E2, GRHL2 can either

867 promote gene transcription by facilitating the recruitment of coregulators like MLL3, or repress gene
868 transcription by repressing coregulators, like p300.

869 **Supplemental Figure 1: Similar patterns of GRHL2 regulation of E2-mediated ER transcriptional activity**
870 **are observed in T47D cells.** A) Representative Western blot of T47D samples used in RNA-seq. Cells
871 were transfected with siCtrl or siGRHL2 and treated for 24 hours with vehicle or 10 nM E2. β-actin is
872 used as a loading control. B) PCA plot of T47D RNA-seq data displaying differences between siCtrl
873 (purple), siGRHL2 (green), vehicle treatment (circles), and E2 treatment (triangles). C) Heatmap showing
874 the expression of ER/GRHL2 co-regulated genes, E2-only regulated genes, and GRHL2-only regulated
875 genes. D) Gene expression profiles of ER/GRHL2 co-regulated gene clusters. Error bars represent mean ±
876 standard error.

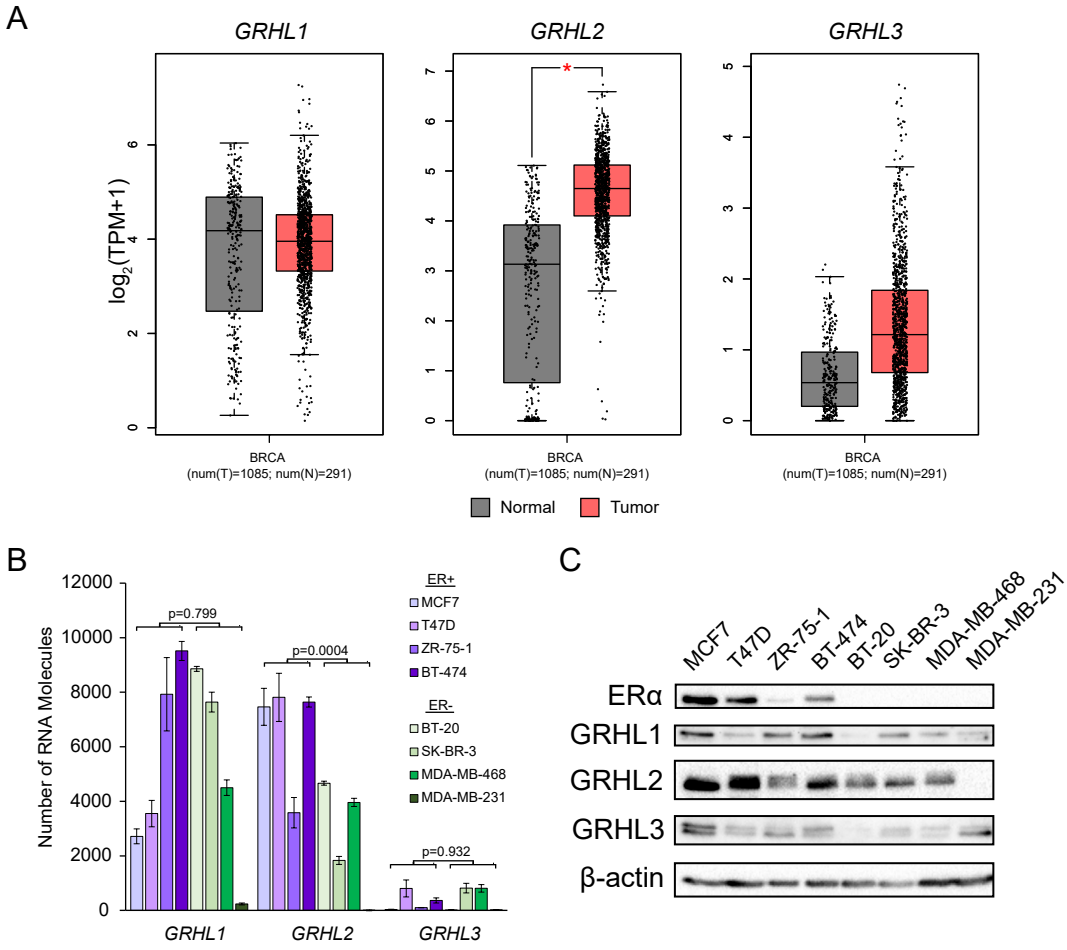

Figure 1: GRHL2 expression is higher in ER-positive vs ER-negative breast cancer. A) mRNA expression of the GRHL family in normal and tumor breast tissue obtained from GEPIA2. A * indicates a p-value < 0.05. B) Absolute quantification of GRHL mRNA and in a panel of ER-positive and ER-negative breast cancer cell lines. Error bars represent mean ± standard error. C) Representative Western blot of GRHL protein levels in the same cell panel. β-actin is used as a loading control.

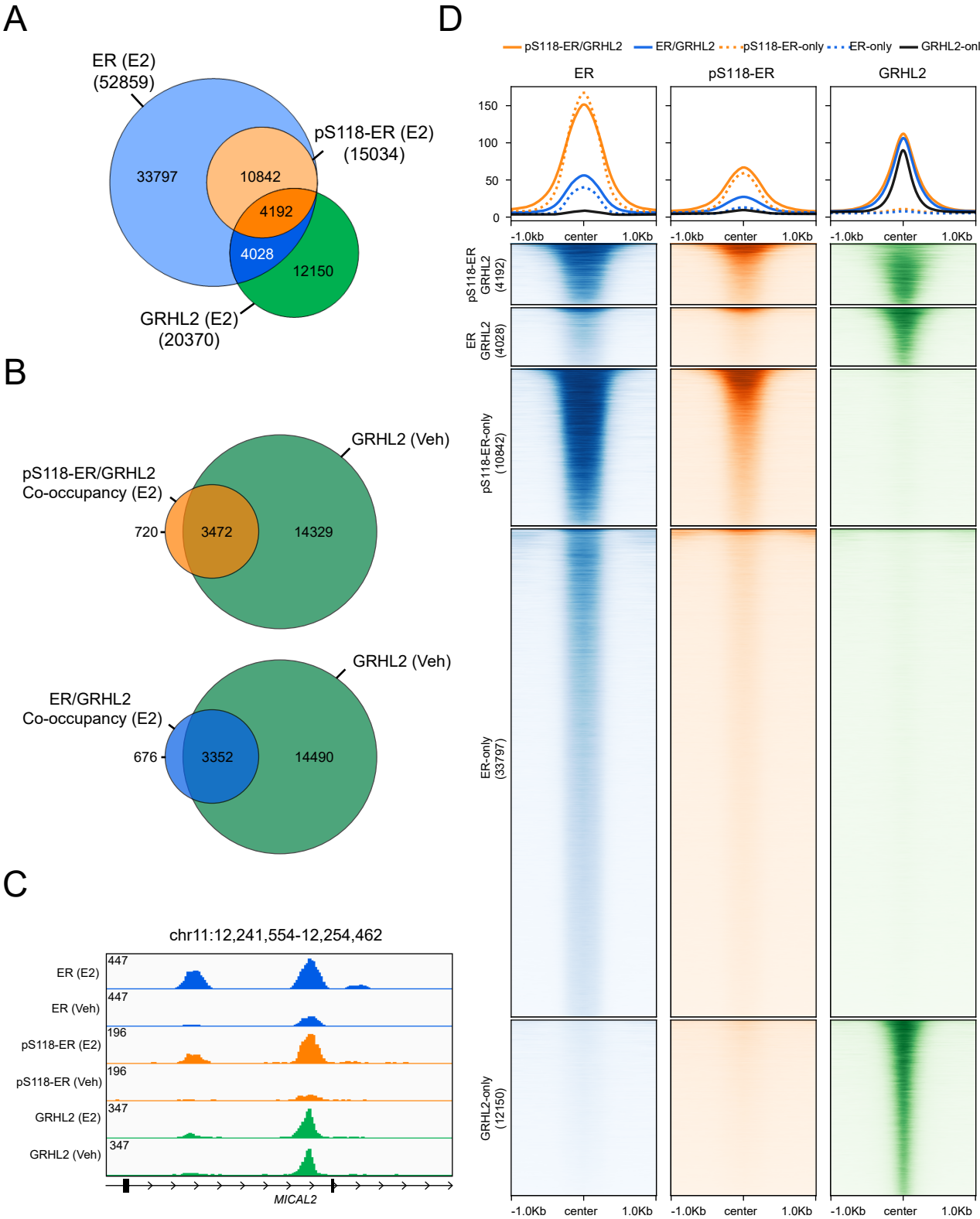

Figure 2: Identification of pS118-ER/GRHL2 co-occupancy sites. A) Venn diagram showing the overlap of MCF7 E2-treated total ER, pS118-ER, and GRHL2 ChIP-seq datasets. pS118-ER binding sites are a subset of total ER bindings sites. ER sites are defined as those that do not overlap with the pS118-ER dataset. Five binding categories were established: pS118-ER/GRHL2 co-occupancy (4,192 sites), ER/GRHL2 co-occupancy (4,028 sites), pS118-ER-only (10,842 sites), ER-only (33,797 sites), and GRHL2-only (12,150 sites). B) Venn diagrams showing the overlap of pS118-ER/GRHL2 co-occupancy sites and ER/GRHL2 co-occupancy sites with GRHL2 peaks detected in vehicle conditions. C) Representative genome browser track of a pS118-ER/GRHL2 co-occupancy site. D) Heatmaps showing binding signal of ER, pS118-ER, and GRHL2 at each of the five binding categories. Data were obtained from previously published ChIP-seq datasets (56).

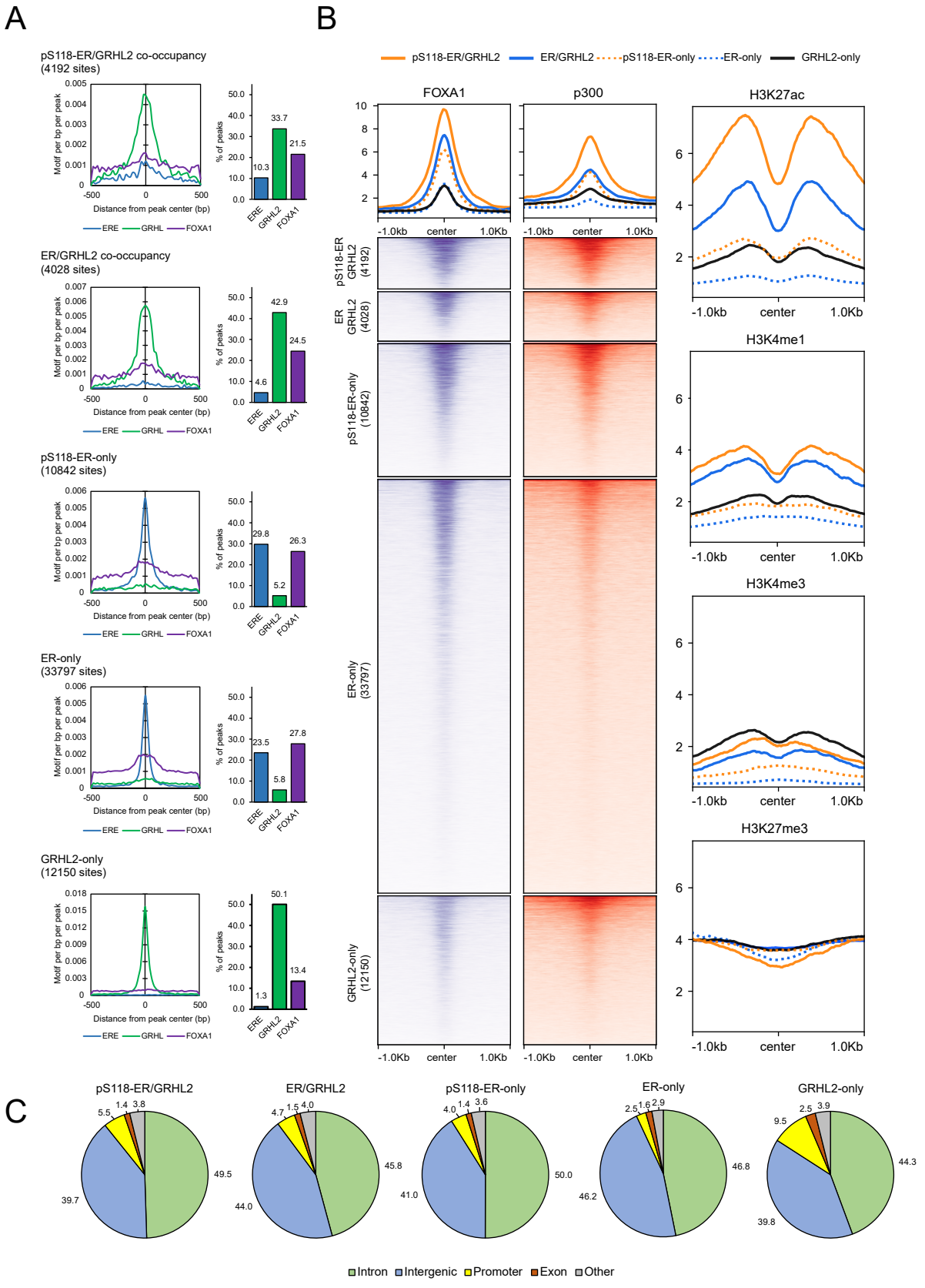

Figure 3: pS118-ER/GRHL2 co-occupancy sites are located at enhancers. A) Motif analysis of the GRHL, ERE, and FOXA1 motifs at co-occupancy sites. The first column shows enrichment of the indicated motif (ERE in blue, GRHL in green, FOXA1 in purple) relative to the peak center. The second column shows the percent of sites with each of the motifs. C) Heatmaps showing binding signal of FOXA1 and p300 and metaplots showing the signal of the histone modifications H3K4me1, H3K4me3, H3K27ac, and H3K27me3 at each of the previously established binding categories. Data were obtained from previously published ChIP-seq datasets (82-85). C) Genome location annotation of the five binding categories. Sites were annotated to introns, intergenic regions, promoters, exons, or other. Promoters were defined as -1kb to +100bp from the transcription start site.

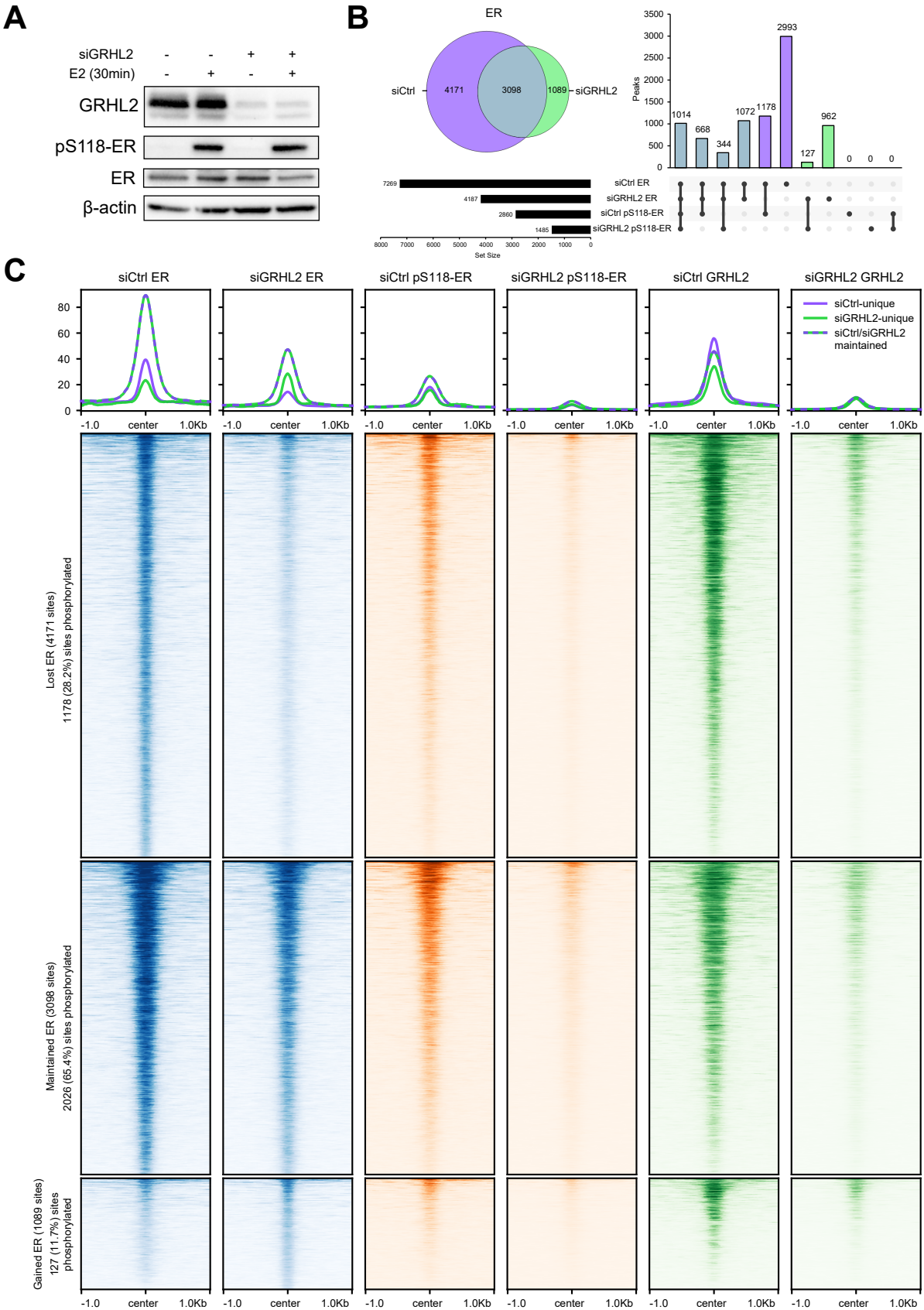

Figure 4: The loss of GRHL2 causes a reduction in ER and pS118-ER chromatin binding. A) Representative western blot of MCF7 samples used in CUT&RUN experiments. Cells were transfected with siCtrl or siGRHL2 and treated for 30 minutes with vehicle or 10 nM E2. β-actin is used as a loading control. B) Venn diagram and upset plot indicating the overlap of ER and pS118-ER CUT&RUN peaks in E2-treated, siCtrl- or siGRHL2-transfected cells. C) Heatmaps showing CUT&RUN signal for ER, pS118-ER, and GRHL2 at lost ER sites (purple), maintained ER siCtrl/siGRHL2 sites (purple and green dashed), and gained ER sites (green). The percent of ER sites detected by the pS118-ER antibody are indicated in region labels.

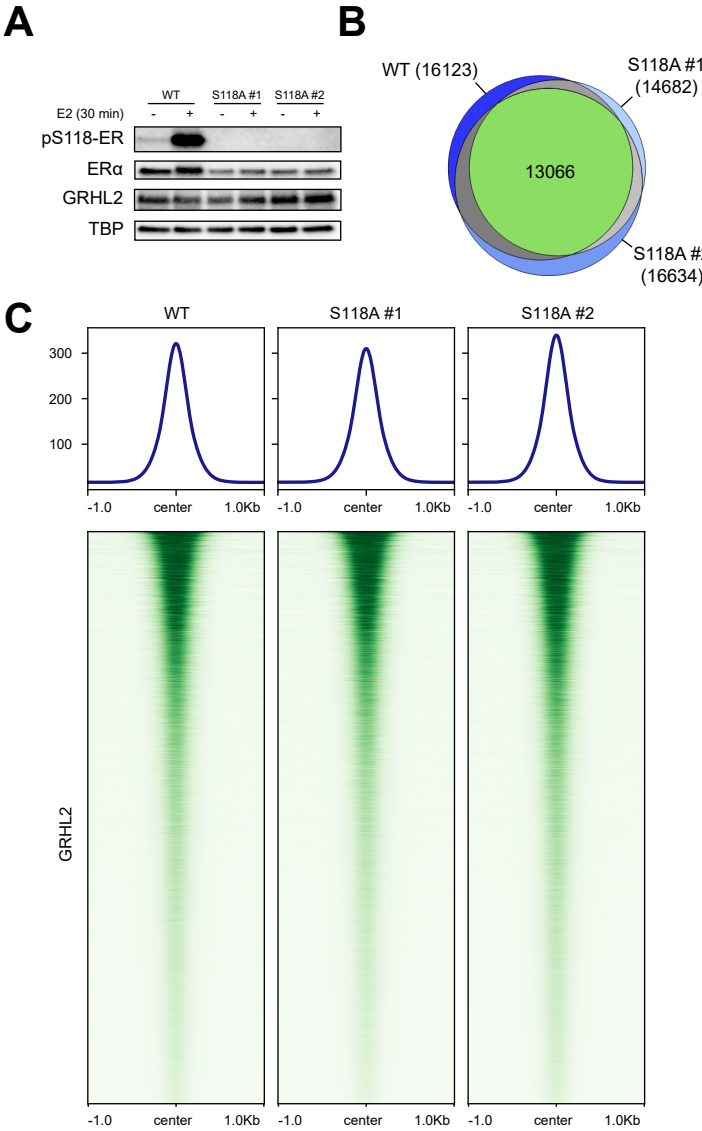

Figure 5: Loss of pS118-ER does not affect GRHL2 chromatin binding. A) Representative western blot of WT and S118A mutant MCF7 cells used for ChIP-seq. Cells were treated for 30min with vehicle or 10 nM E2. TBP is used as a loading control. B) Venn diagrams showing the overlap of E2 GRHL2 binding sites between WT cells and two S118A mutant clones. C) Heatmaps showing GRHL2 binding signal at collective GRHL2 binding sites across all three cell lines.

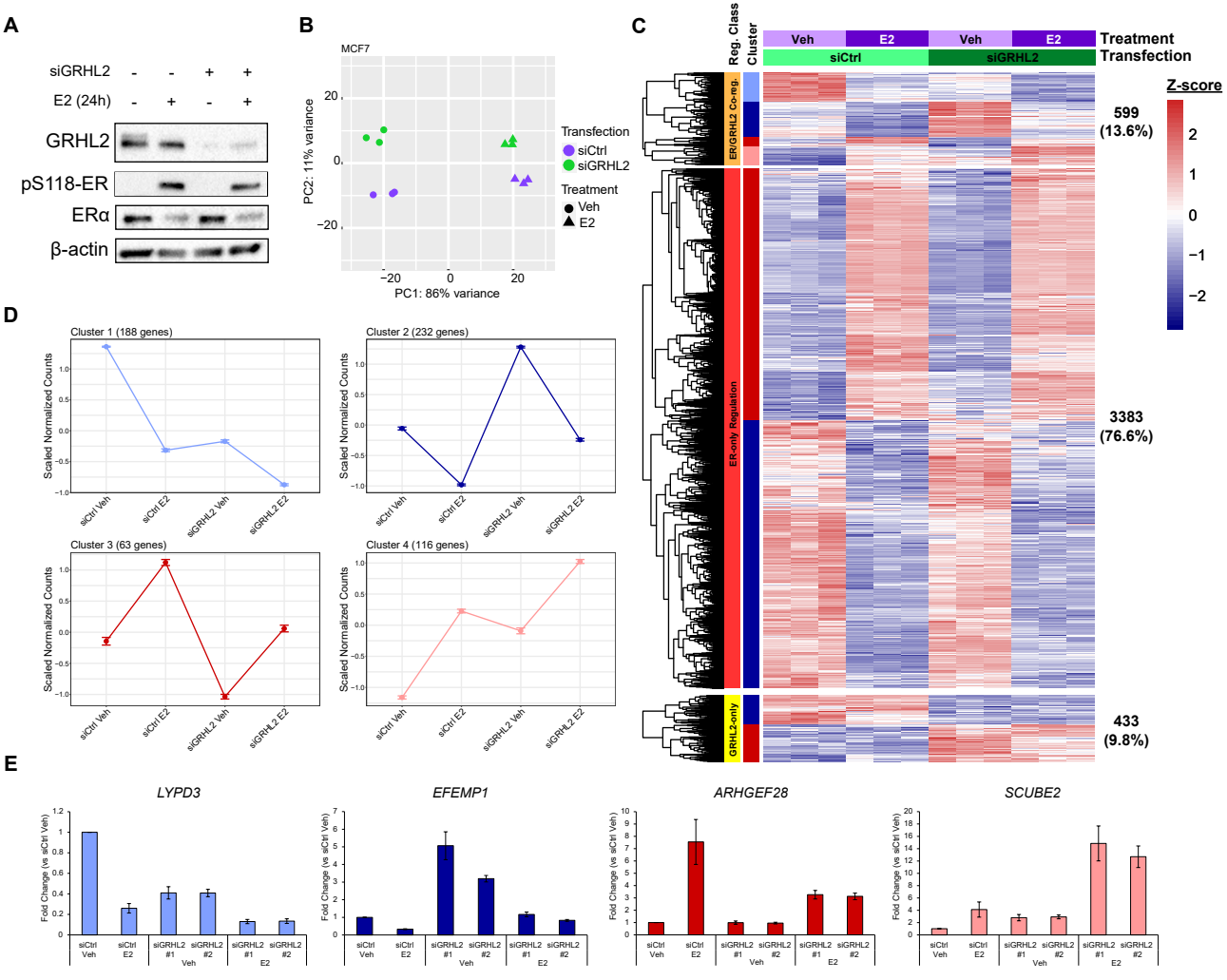

Figure 6: GRHL2 can enhance and antagonize E2-mediated ER transcriptional activity. A) Representative Western blot of MCF7 samples used in RNA-seq. Cells were transfected with siCtrl or siGRHL2 and treated for 24 hours with vehicle or 10 nM E2. β-actin is used as a loading control. B) PCA plot of MCF7 RNA-seq data displaying differences between siCtrl (purple), siGRHL2 (green), vehicle treatment (circles), and E2 treatment (triangles). C) Heatmap showing the expression of ER/GRHL2 co-regulated genes, ER-only regulated genes, and GRHL2-only regulated genes. D) Gene expression profiles of ER/GRHL2 co-regulated gene clusters. Error bars represent mean ± standard error. E) qPCR validation of selected genes from each of the ER/GRHL2 co-regulated gene clusters using two different siRNAs against GRHL2. All values are relative to siCtrl Veh. Error bars represent mean ± standard error.

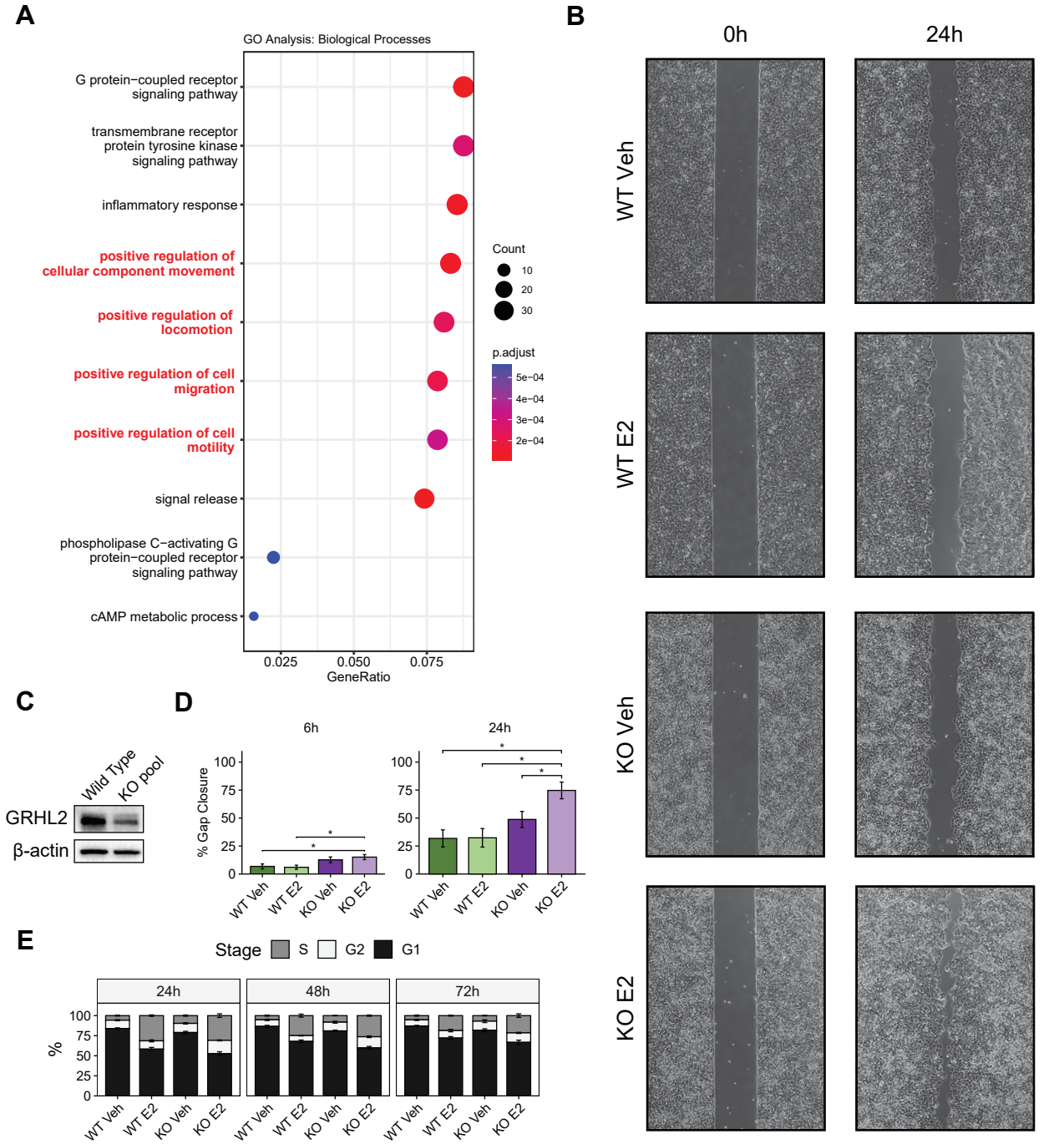

Figure 7: GRHL2 and E2 co-regulate migration. A) Gene ontology analysis for biological processes performed with clusterProfiler on ER/GRHL2 co-regulated genes. Terms related to cell migration, motility, and locomotion are highlighted in red. The size of the dots represents the number of genes annotated to a given term, and color represents the adjusted p-value with red being the most significant. B) Brightfield images of WT and GRHL2-KO cell migration across a cell-free gap over the course of 24 hours. C) Representative Western blot showing the loss of GRHL2 in pooled CRISPR GRHL2-KO cells. D) Quantification of the percent gap closure over 6 hours and 24 hours. Error bars represent mean ± standard error and * indicates a p-value < 0.05. E) Flow cytometry analysis showing the percent of cells in each of the cell cycle stages (S, G2, G1). WT and GRHL2-KO cells were treated with vehicle or 10 nM E2 over 24h, 48h, and 72h. Error bars represent mean ± standard error.

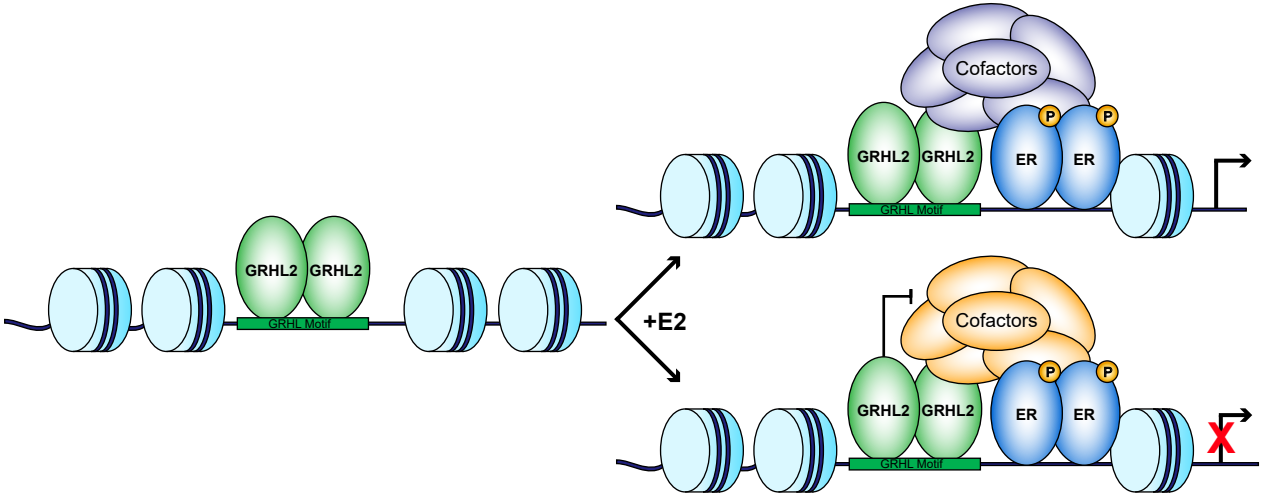

Figure 8: Model of GRHL2 function in facilitating pS118-ER binding and transcriptional activity. GRHL2 binds to the GRHL motif in enhancers prior to ligand treatment. Upon exposure to E2, GRHL2 can either promote gene transcription by facilitating the recruitment of coregulators like MLL3, or repress gene transcription by repressing coregulators, like p300.